Beam normal spin asymmetry for the $ep \to e\Delta(1232)$ process

Carl E. Carlson

College of William and Mary, Physics Department, Williamsburg, Virginia 23187, USA

Barbara Pasquini

Dipartimento di Fisica, Università degli Studi di Pavia, 27100 Pavia, Italy and
INFN Sezione di Pavia, 27100 Pavia, Italy

Vladyslav Pauk

Jefferson Laboratory, Newport News, VA 23606, USA

Marc Vanderhaeghen

Institut für Kernphysik and PRISMA Cluster of Excellence,
Johannes Gutenberg Universität, D-55099 Mainz, Germany
(Dated: December 11, 2017)

We calculate the single spin asymmetry for the $ep \to e\Delta(1232)$ process, for an electron beam polarized normal to the scattering plane. Such single spin asymmetries vanish in the one-photon exchange approximation, and are directly proportional to the absorptive part of a two-photon exchange amplitude. As the intermediate state in such two-photon exchange process is on its mass shell, the asymmetry allows one to access for the first time the on-shell $\Delta \to \Delta$ as well as $N^* \to \Delta$ electromagnetic transitions. We present the general formalism to describe the $ep \to e\Delta$ beam normal spin asymmetry, and provide a numerical estimate of its value using the nucleon, $\Delta(1232)$, $S_{11}(1535)$, and $D_{13}(1520)$ intermediate states. We compare our results with the first data from the Qweak@JLab experiment and give predictions for the A4@MAMI experiment.

I. INTRODUCTION

A lot of information is available on the electromagnetic structure of protons and neutrons, such as their magnetic moments, charge radii, elastic form factors, or electromagnetic polarizabilities. In contrast, our knowledge on the electromagnetic structure of nucleon excited states is very scarce. Even for the lowest excitation of the nucleon, the prominent $\Delta(1232)$ resonance, the information is limited to the non-diagonal $N \to \Delta$ electromagnetic transition, see e.g. Refs. [1–3] for some recent reviews. Deducing from such measurements physical quantities as the magnetic dipole moment or the charge radius of the $\Delta(1232)$ state, has long required resorting to theoretical approaches which relate the properties of the Δ to properties of the nucleon and/or to the experimentally accessible $N \to \Delta$ transition. Such theoretical approaches include different types of constituent quark models (see Ref. [1] for a review of some of these models), general large-N_c relations in QCD [4–7], as well as chiral effective field theory including nucleon and Δ fields [8–12]. In recent years, lattice QCD has been able to also provide direct calculations of such static quantities and FFs for the Δ resonance [13–15].

In order to experimentally access the electromagnetic structure of the $\Delta(1232)$ resonance, and to directly compare with lattice QCD predictions, a way to measure the diagonal $\Delta \to \Delta$ electromagnetic transition is required. As the $\Delta(1232)$ is a very short lived resonance, the only viable way is to use a reaction where the Δ is first produced, and then couples to the electromagnetic field before decaying into a πN state. One such process which

has been proposed to access the magnetic dipole moment (MDM) of the $\Delta^+(1232)$ resonance is the radiative π^0 photoproduction process $\gamma p \to \gamma \Delta^+ \to \gamma \pi^0 p$ [9, 16–20]. A first experimental extraction of the $\Delta^+(1232)$ MDM has been performed in Ref. [21] using the reaction model of Ref. [18], resulting in the value listed by PDG [22]:

$$\mu_{\Delta^+} = 2.7^{+1.0}_{-1.3}(\text{stat.}) \pm 1.5(\text{syst.}) \pm 3(\text{theor.}) \,\mu_N \,, \quad (1)$$

with $\mu_N = e/2M_N$ the nuclear magneton. One notices that the error in Eq. (1) is dominated by the theoretical uncertainty. A dedicated follow-up $\gamma p \to \gamma \pi^0 p$ experiment [23] found it difficult to improve on the precision of the Δ^+ MDM due to model dependencies in the used theoretical framework, which is needed to access the on-shell $\gamma^* \Delta \Delta$ vertex from such reaction process.

Accessing the on-shell electromagnetic FFs of the $\Delta(1232)$ resonance has not been possible in experiment to date. To achieve such goal, we need a two-photon observable where the Δ is firstly produced on a proton target by one virtual photon and then couples to the second photon leading to the Δ final state, which is then detected through its πN decay. In order to properly access the on-shell $\gamma^* \Delta \Delta$ vertex, we need to look at the pole-position of the intermediate Δ state. If we want to realize such an experiment with virtual photons it will in general be dominated by the direct electromagnetic $N \to \Delta$ transition which involves only one photon, and is well studied in experiment, e.g. through the pion electroproduction process on a proton in the Δ region. If we aim to access the electromagnetic Δ FFs, we need an observable where this direct $N \to \Delta$ transition through

one photon is suppressed or absent. An observable which realizes this is the beam normal spin asymmetry for the $ep \rightarrow e\Delta(1232)$ process, which we study in this work.

Normal single spin asymmetries (SSA) for the $ep \rightarrow eR$ processes, with R some well defined state, e.g. reconstructed through its invariant mass, with either the electron beam or the hadronic target polarized normal to the scattering plane, are exactly zero in absence of two or multi-photon exchange contributions. These normal SSAs are proportional to the imaginary (absorptive) part of the two-photon exchange (TPE) amplitude, which is the reason why they are exactly zero for real (non-absorptive) processes such as one-photon exchange (OPE). At leading order in the fine-structure constant, $\alpha = e^2/(4\pi) \simeq 1/137$, the normal SSA results from the product between the OPE amplitude and the imaginary part of the TPE amplitude, see Ref. [24] for a recent review. As the SSA is proportional to the imaginary part of the TPE amplitude at leading order in α, it guarantees that the intermediate hadronic state is produced on its mass shell.

For a target polarized normal to the scattering plane, the corresponding normal SSAs were predicted to be in the (sub) per-cent range some time ago [25]. Recently, a first measurement of the target normal SSA for the elastic electron-^{3}He scattering has been performed by the JLab Hall A Coll., extracting a SSA for the elastic electron-neutron subprocess, for a normal polarization of the neutron, in the per-cent range [26]. For the experiments with polarized beams, the corresponding normal SSAs for the $ep \rightarrow ep$ process involve a lepton helicity flip which is suppressed by the mass of the electron relative to its energy. Therefore these beam normal SSA were predicted to be in the range of a few to hundred ppm for electron beam energies in the GeV range [27–29]. Although such asymmetries are small, the parity violation programs at the major electron laboratories have reached precisions on asymmetries with longitudinally polarized electron beams well below the ppm level, and the next generation of such experiments is designed to reach precisions at the sub-ppb level [30]. The beam normal SSA, which is due to TPE and thus parity conserving, has been measured over the past fifteen years as a spin-off by the parity-violation experimental collaborations at MIT-BATES (SAMPLE Coll.) [31], at MAMI (A4 Coll.) [32, 33], and at JLab (G0 Coll. [34, 35], HAPPEX/PREX Coll. [36], and Qweak Coll. [37]). The measured beam normal SSA for the elastic $ep \rightarrow ep$ process ranges from a few ppm in the forward angular range to around a hundred ppm in the backward angular range, in good agreement with theoretical TPE expectations.

Preliminary results from the QWeak Coll. [38, 39] for the beam normal SSA for the $ep \rightarrow e\Delta^+(1232)$ process indicate that the asymmetry for the inelastic process is around an order of magnitude larger than the elastic asymmetry. It is the aim of this work to detail the formalism to understand this inelastic beam normal spin asymmetries and to study their sensitivity on the

$\Delta(1232)$ electromagnetic FFs as well as on the $N^* \rightarrow \Delta$ electromagnetic transitions.

The outline of this work is as follows. In Section II we briefly recall the definition of the beam normal SSA. In Section III, we describe the leading one-photon exchange amplitude to the $ep \rightarrow e\Delta$ process. Subsequently in Section IV, we give the general expression of the absorptive part of the two-photon exchange amplitude to the $ep \rightarrow e\Delta$ process, and describe the dominant regions in the phase space integrations. In Section V, we provide the details of the model for the hadronic tensor entering the $ep \rightarrow e\Delta$ TPE amplitude which we use in this work. Besides the intermediate nucleon contribution, we subsequently describe the $\Delta(1232)$, $S_{11}(1535)$, and $D_{13}(1520)$ resonance intermediate state contributions. In Section VI, we show our results and discussions. We compare with the existing data for the Qweak@JLab experiment, and provide predictions for the A4@MAMI experiment. Our conclusions are given in Section VII. We provide the quark model relations to relate the electromagnetic $\Delta \rightarrow S_{11}$ and $\Delta \rightarrow D_{13}$ helicity amplitudes to the $N \rightarrow S_{11}$ and $N \rightarrow D_{13}$ helicity amplitudes in an Appendix.

II. BEAM NORMAL SPIN ASYMMETRY

The beam normal single spin asymmetry (B_n), corresponding with the scattering of an electron with polarization *normal* to the scattering plane on a unpolarized proton target, is defined by :

$$B_n = \frac{\sigma_\uparrow - \sigma_\downarrow}{\sigma_\uparrow + \sigma_\downarrow}, \qquad (2)$$

where $\sigma_\uparrow$ ($\sigma_\downarrow$) denotes the cross section for an unpolarized target and for an electron spin parallel (anti-parallel) to the normal polarization vector, defined as :

$$\xi^\mu = (0, \vec{\xi}), \qquad \vec{\xi} \equiv (\vec{k} \times \vec{k}')/|\vec{k} \times \vec{k}'|. \qquad (3)$$

Applying the derivation of Ref. [25] to the case of a beam polarization normal to the scattering plane, B_n can be expressed to order e^2 as:

$$B_n \simeq \frac{2 \, \mathrm{Im} \left[(T_{1\gamma})^*_{fi} \, (\mathrm{Abs} \, T_{2\gamma})_{fi} \right]}{\sum_{\mathrm{spins}} |T_{1\gamma}|^2}, \qquad (4)$$

where $T_{1\gamma}$ denotes the OPE amplitude, and $\mathrm{Abs} T_{2\gamma}$ the absorptive part of the TPE amplitude between the initial state i and the final state f. The beam polarization in the initial state in Eq. (4) is understood along the direction of $\vec{\xi}$. The numerator in Eq. (4) corresponds (to order e^2) to the difference of squared amplitudes for normal beam polarizations $\uparrow$ and $\downarrow$, while all other spins are summed over, whereas the denominator is the squared amplitude summed over all spins. The phase of the amplitude T is defined through its relation to the S-matrix amplitude

$S = 1 - iT$. In Eq. (4), the absorptive part of the two-photon amplitude is defined as [1]:

$$(\text{Abs}\, T_{2\gamma})_{fi} \equiv \sum_n T_{nf}^* \, T_{ni}, \qquad (5)$$

involving a sum over all physical (i.e. on-shell) intermediate states n.

Generally, as illustrated by Eq. (4), one-photon exchange alone will give no beam normal single spin asymmetry. The observed particle needs at least one further interaction. When only the final electron is observed, which we consider in this work, this means two or more photon exchange. In the resonance region, one can imagine observing instead a final pion, whence a non-zero B_n is possible even for one-photon exchange [40], since the strong force guarantees final state interactions for the pion.

In the following, we will evaluate Eq. (4) for the $e^- p \to e^- \Delta(1232)$ process. To this aim, we will discuss in Section III the OPE amplitude $T_{1\gamma}$, and in Sections IV and V the absorptive part of the TPE amplitude.

III. ONE-PHOTON EXCHANGE AMPLITUDE

In this section, we briefly review the inelastic $ep \to e\Delta$ process in the one-photon exchange (OPE) approximation. The kinematics of the inelastic transition :

$$e^-(k, s_e) + N(p, \lambda) \to e^-(k', s_e') + \Delta(p', \lambda'), \qquad (6)$$

is described by four-vectors $k(k')$ of the initial (final) electrons, and $p(p')$ of the nucleon (Δ). Furthermore, $s_e(s_e')$ denote the normal spin projections of the initial (final) electrons, and $\lambda(\lambda')$ the helicities of the nucleon (Δ). In this work, we will use the notation q for the momentum transfer towards the hadronic system:

$$q = k - k' = p' - p, \qquad (7)$$

and adopt the usual definitions for the kinematical invariants of this process:

$$s = (k+p)^2, \quad u = (k - p')^2, \quad t = q^2 \equiv -Q^2, \qquad (8)$$

which are related as: $s + u - Q^2 = M_N^2 + M_\Delta^2 + 2m_e^2$, where $M_N(M_\Delta)$ are the nucleon (Δ) masses respectively, and m_e is the electron mass. Usually experiments are performed at fixed beam energy E_e, which determines s as $s = M_N^2 + m_e^2 + 2M_N E_e$. Furthermore, it is conventional in electron scattering to introduce the polarization parameter ε of the virtual photon, which can be expressed in terms of the above kinematical invariants as (neglect-

ing the electron mass):

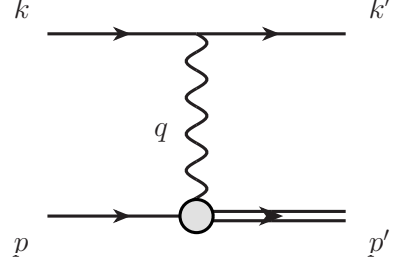$$\varepsilon = \frac{2(M_N^2 M_\Delta^2 - su)}{s^2 + u^2 - 2M_N^2 M_\Delta^2}. \qquad (9)$$

Figure 1. The one-photon exchange diagram. The grey blob represents the electromagnetic vertex of the nucleon.

The OPE amplitude for the $ep \to e\Delta$ process is given by [2]:

$$T_{1\gamma} = -\frac{e^2}{Q^2} \bar{u}(k', s_e')\gamma_\mu u(k, s_e)\langle \Delta(p', \lambda')|J^\mu(0)|N(p, \lambda)\rangle, \qquad (10)$$

with e the proton electric charge. The matrix element of the hadronic current can be expressed in the covariant form :

$$\langle \Delta(p', \lambda')|J^\mu(0)|N(p, \lambda)\rangle \equiv \bar{u}_\alpha(p', \lambda')\Gamma_{N\Delta}^{\alpha\mu}(p', p)u(p, \lambda), \qquad (11)$$

where u is the nucleon spinor, and u_α is the Rarita-Schwinger spinor for the Δ. Furthermore, the on-shell $\gamma^* N\Delta$ vertex is given by:

$$\begin{aligned}
\Gamma_{N\Delta}^{\alpha\mu}(p', p) \equiv \sqrt{\frac{3}{2}} \frac{(M_\Delta + M_N)}{M_N Q_{N\Delta+}^2} \Big[& g_M(Q^2)i\,\varepsilon^{\alpha\mu\rho\sigma} p_\rho' q_\sigma \\
& - g_E(Q^2)(q^\alpha p'^\mu - q\cdot p' g^{\alpha\mu})\gamma_5 \\
& - g_C(Q^2)(q^\alpha q^\mu - q^2 g^{\alpha\mu})\gamma_5 \Big], \qquad (12)
\end{aligned}$$

where we use $\varepsilon_{0123} = +1$, and where g_M, g_E, and g_C represent the three form factors (FFs) describing the $N \to \Delta$ vector transition [1]. We furthermore introduced the shorthand notation:

$$Q_{N\Delta\pm}^2 \equiv Q^2 + (M_\Delta \pm M_N)^2. \qquad (13)$$

Phenomenologically, the $\gamma^* N\Delta$ transition is usually expressed in terms of a different set of FFs introduced by Jones-Scadron [41], which are labeled G_M^*, G_E^*, G_C^*, and

---

[1] With this definition, one obtains the absorptive part from unitarity as: $\text{Abs}\, T_{fi} = i\left[(T)_{fi} - (T^\dagger)_{fi}\right]$.

---

[2] For simplicity of notation, we will redefine here and in the following of the paper the T-matrix elements by taken a global energy-momentum conservation factor $(2\pi)^4\delta^4(k + p - k' - p')$ out of the T-matrix element.

describe the magnetic dipole (M1), electric quadrupole (E2), and Coulomb quadrupole (C2) transitions respectively. The latter have the property that they have a one-to-one relation with the imaginary parts of the pion electroproduction multipoles at the resonance position, and have been extracted in experiment, see Ref. [1] for details. In terms of these Jones-Scadron FFs, the FFs entering Eq. (12) are straightforwardly related as:

$$g_M = G_M^* - G_E^*, \tag{14}$$

$$g_E = -\frac{2}{Q_{N\Delta-}^2}\left[(M_\Delta^2 - M_N^2 - Q^2)G_E^* + Q^2 G_C^*\right],$$

$$g_C = \frac{1}{Q_{N\Delta-}^2}\left[4M_\Delta^2 G_E^* - (M_\Delta^2 - M_N^2 - Q^2)G_C^*\right],$$

where all FFs are functions of Q^2. The spin averaged squared matrix element for the $ep \to e\Delta$ process in the OPE approximation can then be expressed as:

$$\sum_{\text{spins}} |T_{1\gamma}|^2 \equiv \frac{e^4}{Q^2} D_{1\gamma}(s, Q^2), \tag{15}$$

where the function $D_{1\gamma}(s, Q^2)$ is given by:

$$D_{1\gamma}(s, Q^2) = \frac{2\,Q_{N\Delta-}^2\,(M_\Delta + M_N)^2}{(1-\varepsilon)\,M_N^2}$$
$$\times \left[G_M^{*2} + 3G_E^{*2} + \varepsilon\frac{Q^2}{M_\Delta^2}G_C^{*2}\right]. \tag{16}$$

In this work, we will take the empirical information on the FFs $G_M^*(Q^2)$, $G_E^*(Q^2)$, and $G_C^*(Q^2)$, characterizing the electromagnetic $N \to \Delta$ transition, from the MAID2007 analysis [42, 43]. In this analysis, the empirical $N \to \Delta$ transition FFs have been expressed as:

$$G_{M,E,C}^*(Q^2) = \left(\frac{Q_{N\Delta+}}{M_N + M_\Delta}\right)G_{M,E,C}^{*\,Ash}(Q^2), \tag{17}$$

with the so-called Ash FFs $G_{M,E,C}^{*\,Ash}$ parameterized as [42, 43]:

$$G_M^{*\,Ash}(Q^2) = 3.00(1 + 0.01Q^2)e^{-0.23Q^2}G_D(Q^2),$$
$$G_E^{*\,Ash}(Q^2) = 0.064(1 - 0.021Q^2)e^{-0.16Q^2}G_D(Q^2),$$
$$G_C^{*\,Ash}(Q^2) = 0.124\frac{(1 + 0.120Q^2)}{1 + 4.9Q^2/(4M_N^2)}\left(\frac{4M_\Delta^2}{M_\Delta^2 - M_N^2}\right)$$
$$\times e^{-0.23Q^2}G_D(Q^2), \tag{18}$$

for Q^2 in GeV^2, and where $G_D(Q^2) = 1/(1 + Q^2/0.71)^2$ is the standard dipole FF. Note that the magnetic dipole $N \to \Delta$ transition provides by far the dominant contribution as $G_M^*(0) = 3.0$, whereas the electric and Coulomb quadrupole FFs are only at the few percent level relative to the magnetic dipole FF in the low Q^2 range.

We like to notice that in the forward direction, $Q^2 \to 0$, the function $D_{1\gamma}$ for the $ep \to e\Delta$ process behaves, for fixed beam energy, approximately as:

$$D_{1\gamma} \xrightarrow[Q^2 \to 0]{} \frac{4}{M_N^2}\left\{\left(s - \frac{1}{2}(M_\Delta^2 + M_N^2)\right)^2\right.$$
$$\left. + \frac{1}{4}(M_\Delta^2 - M_N^2)^2\right\}\left[G_M^{*2} + 3G_E^{*2}\right]. \tag{19}$$

In contrast, the corresponding function for the elastic process $ep \to ep$, which we denote by $D_{1\gamma}^{el}$, behaves as [29]:

$$D_{1\gamma}^{el} \xrightarrow[Q^2 \to 0]{} \frac{16}{Q^2}(s - M_N^2)^2 F_1^2$$
$$+ \frac{4}{M_N^2}\left[(s - M_N^2)^2 F_2^2 - 4sM_N^2 F_1^2\right] + \mathcal{O}(Q^2), \tag{20}$$

where F_1 (F_2) are the Dirac (Pauli) FFs of the nucleon respectively. Eq. (20) then leads at forward angles to the characteristic $1/Q^4$ Rutherford behavior for the elastic OPE squared amplitude, defined by Eq. (15). On the other hand, the $ep \to e\Delta$ process, which necessarily involves a finite energy and momentum transfer, behaves as the Pauli (F_2) FF term of the elastic process, which only leads to a $1/Q^2$ behavior for the squared amplitude at small Q^2. We therefore see that the OPE cross section for the $ep \to e\Delta$ process, which enters the denominator of B_n, is suppressed by one power of Q^2 relative to its elastic counterpart. The TPE amplitude for the $ep \to e\Delta$ process, on the other hand, does not have this same suppression at forward angles, as we will see in the following. As B_n is proportional to the TPE amplitude relative to the OPE amplitude, see Eq. (4), this leads to an enhancement of B_n for the $ep \to e\Delta$ process at small values of Q^2, relative to its elastic counterpart.

IV. IMAGINARY (ABSORPTIVE) PART OF THE TWO-PHOTON EXCHANGE AMPLITUDE

In this section we relate the imaginary part of the TPE amplitude, which appears in the numerator of B_n, to the absorptive part of the matrix element for the $ep \to e\Delta$ process, as shown in Fig. 2.

In the e^-p c.m. frame, its contribution can be expressed as:

$$\text{Abs } T_{2\gamma} = \int \frac{d^3\vec{l}}{(2\pi)^3 2E_l}\bar{u}(k', s_e')\gamma_\mu(\gamma \cdot l + m_e)\gamma_\nu u(k, s_e)$$
$$\times \frac{e^4}{Q_1^2 Q_2^2} \cdot W^{\mu\nu}(p', \lambda'; p, \lambda), \tag{21}$$

where the momenta are defined as indicated on Fig. 2, with $q_1 \equiv k - l$, $q_2 \equiv k' - l$, $q_1 - q_2 = q$, and where E_l is the energy of the intermediate lepton. Furthermore, $Q_1^2 \equiv -q_1^2 = -(k - l)^2$ and $Q_2^2 \equiv -q_2^2 = -(k' - l)^2$ correspond with the virtualities of the two spacelike photons. Denoting the c.m. angle between initial and final electrons as θ_{cm}, the momentum transfer $Q^2 \equiv -q^2 > 0$ can
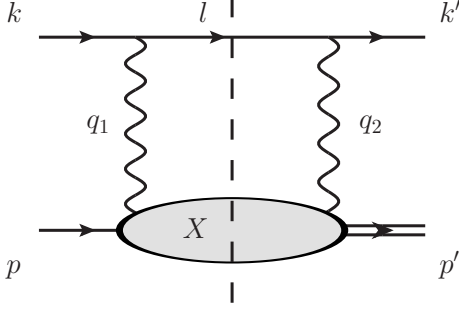
Figure 2. The discontinuity of the two-photon exchange diagram. The cut blob represents the absorptive part of the doubly virtual Compton amplitude on a nucleon.

be expressed as :

$$Q^2 = \frac{(s - M_N^2)(s - M_\Delta^2)}{2\,s}\,(1 - \cos\theta_{cm})\, +\, \mathcal{O}(m_e^2) \quad (22)$$

In Eq. (21), the hadronic tensor $W^{\mu\nu}(p', \lambda'; p, \lambda)$ corresponds with the absorptive part of the doubly virtual $\gamma^* N \to \gamma^* \Delta$ tensor for two *space-like* photons :

$$W^{\mu\nu}(p', \lambda'; p, \lambda) = \sum_X (2\pi)^4\, \delta^4(p + q_1 - p_X)$$
$$\times \langle \Delta(p', \lambda')| J^{\dagger\mu}(0)|X \rangle\, \langle\, X |J^\nu(0)|N(p, \lambda)\rangle, \quad (23)$$

where the sum goes over all possible *on-shell* intermediate hadronic states X. We will use the unitarity relation to express the full non-forward tensor in terms of electroproduction amplitudes $\gamma^* N \to X$. The number of intermediate states X which one considers in the calculation will then put a limit on how high in energy one can reliably calculate the hadronic tensor of Eq. (23). In this work, we will model the tensor $W^{\mu\nu}$ as a sum over different baryon intermediate states, and will explicitly consider $X = N$, $\Delta(1232)$, $S_{11}(1535)$, and $D_{13}(1520)$, resonance contributions.

The phase space integral in Eq. (21) runs over the 3-momentum of the intermediate (on-shell) electron. Evaluating the process in the $e^- p$ c.m. system, we can express the c.m. momentum of the intermediate electron as :

$$|\vec{l}|^2 = \frac{1}{4s}\left[(\sqrt{s} - m_e)^2 - W^2\right]\left[(\sqrt{s} + m_e)^2 - W^2\right],$$
$$(24)$$

where $W^2 \equiv p_X^2$ is the squared invariant mass of the intermediate state X. The c.m. momenta of the initial (and final) electrons are given by the analogous expression as Eq. (24) by replacing W^2 with M_N^2 (M_Δ^2) respectively. The phase space integral in Eq. (21) depends, besides the magnitude $|\vec{l}|$, upon the solid angle of the intermediate electron. We define the polar c.m. angle θ_1 of the intermediate electron w.r.t. to the direction of the initial electron. The azimuthal angle ϕ_1 is chosen such that $\phi_1 = 0$ corresponds with the scattering plane of the $ep \to e\Delta$ process. Having defined the kinematics of the

intermediate electron, we can express the virtuality of both exchanged photons. The virtuality of the photon with four-momentum q_1 is given by :

$$Q_1^2 = \frac{1}{2s}\Big[(s - M_N^2 + m_e^2)(s - W^2 + m_e^2) - 4m_e^2 s$$
$$- \sqrt{(s - M_N^2 + m_e^2)^2 - 4m_e^2 s}$$
$$\times \sqrt{(s - W^2 + m_e^2)^2 - 4m_e^2 s}\,\cos\theta_1\Big]. \quad (25)$$

The virtuality Q_2^2 of the second photon has an analogous expression as Eq. (25) with the replacements $M_N \to M_\Delta$ and $\cos\theta_1 \to \cos\theta_2$, where θ_2 is the angle between the intermediate and final electrons. In terms of the polar and azimuthal angles θ_1 and ϕ_1 of the intermediate electron, one can express :

$$\cos\theta_2\,=\,\sin\theta_{cm}\,\sin\theta_1\,\cos\phi_1\,+\,\cos\theta_{cm}\,\cos\theta_1. \quad (26)$$

In case the intermediate electron is collinear with the initial electron (i.e. for $\theta_1 \to 0$, $\phi_1 \to 0$), denoting the virtual photon virtualities for this kinematical situation by $Q_{i,VCS}^2 \equiv Q_i^2(\theta_1 = 0, \phi_1 = 0)$, one obtains from Eq. (25) that:

$$Q_{1,VCS}^2 \simeq m_e^2 \frac{(W^2 - M_N^2)^2}{(s - W^2)(s - M_N^2)},$$
$$Q_{2,VCS}^2 \simeq \frac{(s - W^2)}{(s - M_N^2)}Q^2 + \mathcal{O}(m_e^2). \quad (27)$$

We thus see that when the intermediate and initial electrons are collinear, the photon with momentum $\vec{q}_1 = \vec{k} - \vec{k}_1$ is also collinear with this direction, and its virtuality becomes of order of $\mathcal{O}(m_e^2)$, whereas the other photon has a large virtuality, of order Q^2. For the case $W = M_N$, this precisely corresponds with the situation where the first photon is soft (i.e. $q_1 \to 0$), and where the second photon carries the full momentum transfer $Q_2^2 \simeq Q^2$. For the case $W > M_N$, the first photon is hard but becomes quasi-real (i.e. $Q_1^2 \sim m_e^2$). In this case, the virtuality of the second photon is smaller than Q^2. An analogous situation occurs when the intermediate electron is collinear with the final electron (i.e. $\theta_2 \to 0$, $\phi_1 \to 0$, which is equivalent with $\theta_1 \to \theta_{cm}$). The corresponding photon virtualities are obtained from Eq. (27) by the replacements $Q_{1,VCS}^2 \leftrightarrow Q_{2,VCS}^2$ and $M_N \leftrightarrow M_\Delta$. The second photon is quasi-real in this case, and the first photon carries a virtuality smaller than Q^2. For the special case of a Δ intermediate state $W = M_\Delta$, the second photon becomes soft, and the first photon carries the full momentum transfer Q^2. These phase space regions with one quasi-real photon and one virtual photon correspond with quasi virtual Compton scattering (quasi-VCS), and correspond at the lepton side with the Bethe-Heitler process, see e.g. Ref. [44] for details. They lead to large enhancements in the integrand entering the absorptive part of the TPE amplitude.

Besides the near singularities corresponding with

quasi-VCS, where the intermediate electron is collinear with either the incoming or outgoing electrons, the TPE process also has a near singularity when the intermediate electron momentum goes to zero $|\vec{l}| \to 0$ (i.e. the intermediate electron is soft). In this case the first photon takes on the full momentum of the initial electron, i.e. $\vec{q}_1 \to \vec{k}$, whereas the second photon takes on the full momentum of the final electron, i.e. $\vec{q}_2 \to \vec{k}'$. One immediately sees from Eq. (24) that this situation occurs when the invariant mass of the hadronic state takes on its maximal value $W = W_{max} \equiv \sqrt{s} - m_e$. In this case, the photon virtualities are given by :

$$Q^2_{1,\,RCS} = \frac{m_e}{\sqrt{s}} \left\{ \left(\sqrt{s} - m_e \right)^2 - M_N^2 \right\},$$

$$Q^2_{2,\,RCS} = \frac{m_e}{\sqrt{s}} \left\{ \left(\sqrt{s} - m_e \right)^2 - M_\Delta^2 \right\}. \qquad (28)$$

This kinematical situation with two quasi-real photons, corresponding with quasi-real Compton scattering (quasi-RCS), also leads to an enhancement in the corresponding integrand of $\mathrm{Abs}\,T_{2\gamma}$.

In the upper panel of Fig. 3, we show the kinematical accessible regions for the virtualities Q_1^2, Q_2^2 in the phase space integral of Eq. (21) for a beam energy of $E_e = 0.855$ GeV corresponding with the A4@MAMI experiment, for different values of the *c.m.* angle θ_{cm}. In the lower panel we display these phase space regions for three different values of W, corresponding with the N, $\Delta(1232)$, and $S_{11}(1535)$ intermediate states. We notice from Fig. 3 that the largest possible photon virtualities in the TPE amplitude occur for the nucleon intermediate state, whereas for the $S_{11}(1535)$ intermediate state both photons have very small virtualities.

Using Eq. (21) for the absorptive part of the TPE amplitude, and Eqs. (10,11) for the OPE amplitude, we can then express the normal spin asymmetry B_n of Eq. (4) for the $ep \to e\Delta$ process in terms of a 3-dimensional phase-space integral:

$$B_n = -\frac{e^2}{D_{1\gamma}(s,Q^2)} \frac{1}{(2\pi)^3} \int_{M^2}^{(\sqrt{s}-m_e)^2} dW^2 \left(\frac{s - W^2}{8\,s} \right)$$

$$\times \int d\Omega_1 \frac{1}{Q_1^2 Q_2^2} \mathrm{Im} \left(L_{\kappa\mu\nu} H^{\kappa\mu\nu} \right), \qquad (29)$$

where the denominator factor $D_{1\gamma}(s,Q^2)$ is originating from the OPE process as given by Eq. (16), and $d\Omega_1 = d\cos\theta_1 d\phi_1$.

The integrand in Eq. (29) arising from the interference between the OPE and TPE amplitudes has been expressed as a product of a lepton tensor $L_{\lambda\mu\nu}$ and a hadron tensor $H^{\lambda\mu\nu}$. The polarized lepton tensor can be expressed as a trace using the spin projection technique:

$$L_{\kappa\mu\nu} = \mathrm{Tr}\{\gamma_\kappa(\slashed{k}' + m_e)\gamma_\mu(\slashed{l} + m_e)\gamma_\nu \gamma_5 \slashed{\xi}(\slashed{k} + m_e)\}, \quad (30)$$

where ξ^α is the polarization vector of Eq. (3) for an electron polarized normal to the scattering plane. We see from Eq. (30) that the polarized lepton tensor vanishes
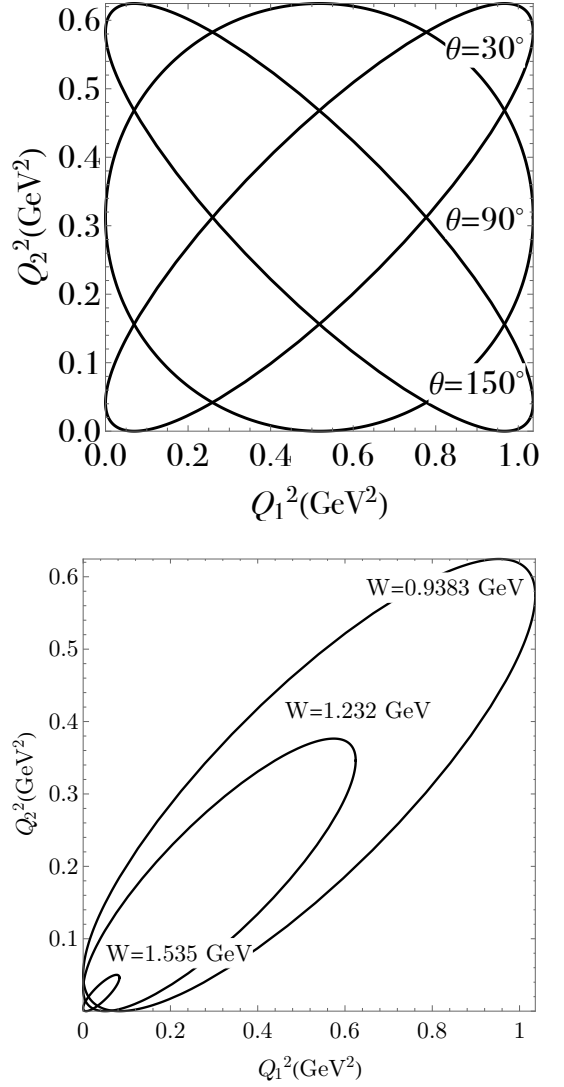

Figure 3. Kinematical accessible region for the virtualities Q_1^2, Q_2^2 in the phase space integral of Eqs. (21, 29) entering the $ep \to e\Delta$ process. The upper panel shows the phase space regions for different *c.m.* angles θ_{cm} as indicated on the ellipses for $E_e = 0.855$ GeV ($s = 2.485$ GeV^2), and for $W = 0.9383$ GeV (i.e. for a nucleon intermediate state). The lower panel shows the allowed values of the photon virtualities for different intermediate states for $\theta_{cm} = 30^o$. We show three cases corresponding with the contribution of N, $\Delta(1232)$ and $S_{11}(1535)$ excitations. The accessible regions correspond with the interior of the ellipses. The intersection with the axes correspond with quasi-VCS, whereas the situation at $W = \sqrt{s} - m_e$ where all ellipses shrink to the point $Q_1^2 = Q_2^2 \simeq 0$ corresponds with quasi-RCS.

for massless electrons. Keeping only the leading term in m_e, it is given by:

$$L_{\kappa\mu\nu} = m_e \left(-\mathrm{Tr}\{\gamma_5 \gamma_\mu \slashed{l}\gamma_\nu \slashed{\xi} \slashed{k} \gamma_\kappa\} + \mathrm{Tr}\{\gamma_5 \slashed{k}' \gamma_\mu \slashed{l}\gamma_\nu \slashed{\xi} \gamma_\kappa\} \right.$$

$$\left. - \mathrm{Tr}\{\gamma_5 \slashed{k}' \gamma_\mu \gamma_\nu \slashed{\xi} \slashed{k} \gamma_\kappa\} \right) + \mathcal{O}(m_e^2). \qquad (31)$$

Furthermore, the unpolarized hadron tensor $H^{\lambda\mu\nu}$ is

given by

$$H^{\kappa\mu\nu} = \sum_{\lambda,\lambda'} [\bar{u}_\alpha(p',\lambda')\Gamma^{\alpha\kappa}_{N\Delta}(p',p)u(p,\lambda)]^*$$
$$\times W^{\mu\nu}(p',\lambda';p,\lambda). \qquad (32)$$

Equivalently, the phase space integration in Eq. (29) can be re-expressed in a Lorentz invariant way as an integral over photon virtualities Q_1^2 and Q_2^2 by using the Jacobian

$$J = \left| \frac{\partial Q_1^2}{\partial\cos\theta_1} \frac{\partial Q_2^2}{\partial\phi_1} \right|. \qquad (33)$$

Using Eq.(25) and an analogous expression for Q_2^2, the Jacobian is given by

$$J = \left[(s - W^2 + m_e^2)^2 - 4m_e^2 s \right] / (4s^2)$$
$$\times \left[(s - M_N^2 + m_e^2)^2 - 4m_e^2 s \right]^{1/2}$$
$$\times \left[(s - M_\Delta^2 + m_e^2)^2 - 4m_e^2 s \right]^{1/2}$$
$$\times \sin\theta_{cm}\sin\theta_1\sin\phi_1, \qquad (34)$$

leading to the equivalent expression for B_n:

$$B_n = -\frac{e^2}{D_{1\gamma}(s,Q^2)} \frac{1}{(2\pi)^3} \int_{M^2}^{(\sqrt{s}-m_e)^2} dW^2 \left(\frac{s-W^2}{8\,s} \right)$$
$$\times \int dQ_1^2 dQ_2^2 \frac{J^{-1}(Q_1,Q_2)}{Q_1^2\,Q_2^2} \mathrm{Im}\left(L_{\kappa\mu\nu} H^{\kappa\mu\nu} \right), \qquad (35)$$

where the (Q_1^2, Q_2^2) integration regions cover the inside of ellipses as displayed in Fig. 3.

We can express the sum over the hadron spins in Eq. (32) as a trace by expressing the hadron tensor $W^{\mu\nu}$ through an operator $\hat{W}$ in spin space, defined as:

$$W^{\mu\nu}(p',\lambda';p,\lambda) \equiv \bar{u}_\beta(p',\lambda')\hat{W}^{\beta\mu\nu}(p',p)u(p,\lambda). \qquad (36)$$

The spin summation in Eq. (32) can then be worked out as:

$$H^{\kappa\mu\nu} = \mathrm{Tr}\left\{ \tilde{\Gamma}^{\alpha\kappa}_{N\Delta}(p',p)P^{(3/2)}_{\alpha\beta}(p',M_\Delta)\hat{W}^{\beta\mu\nu}(p',p) \right.$$
$$\left. \times P^{(1/2)}(p,M_N) \right\}, \qquad (37)$$

where $\tilde{\Gamma}^{\alpha\beta}_{N\Delta} \equiv \gamma^0 \left(\Gamma^{\alpha\beta}_{N\Delta} \right)^\dagger \gamma^0$ stands for the adjoint operator, and where the spin-3/2 and spin-1/2 projectors for a state of mass M are defined by:

$$P^{(1/2)}(p,M) = \not{p} + M, \qquad (38)$$

$$P^{(3/2)}_{\alpha\beta}(p,M) = (\not{p}+M)\left[-g_{\alpha\beta} + \frac{1}{3}\gamma_\alpha\gamma_\beta \right.$$
$$\left. + \frac{1}{3p^2}(\not{p}\gamma_\alpha p_\beta + p_\alpha\gamma_\beta\not{p}) \right]. \qquad (39)$$

For narrow intermediate states X, which we will con-

sider in the following, the hadronic tensor is given by :

$$H^{\kappa\mu\nu} \equiv \sum_X H_X^{\kappa\mu\nu} = \sum_X 2\pi\delta(W^2 - M_X^2)\tilde{H}_X^{\kappa\mu\nu}, \quad (40)$$

where H_X stands for the contribution from each individual state X, and where we have defined $\tilde{H}_X$ by removing a δ-function in invariant mass for each contributing resonance. Using Eq. (40) allows reducing the expression for B_n in Eq. (35) to a 2-dimensional integral:

$$B_n = -\frac{1}{(2\pi)^2} \frac{e^2}{D_{1\gamma}(s,Q^2)} \sum_X \left(\frac{s - M_X^2}{8\,s} \right) \theta(s - M_X^2)$$
$$\times \int dQ_1^2 dQ_2^2 \frac{J^{-1}(Q_1,Q_2)}{Q_1^2\,Q_2^2} \mathrm{Im}\left(L_{\kappa\mu\nu}\tilde{H}_X^{\kappa\mu\nu} \right). \quad (41)$$

V. MODELS FOR THE HADRONIC TENSOR

In this Section, we will model the hadronic tensor $\hat{W}^{\beta\mu\nu}$ of Eq. (36) as a sum over different baryon intermediate states. We will explicitly consider $X = N$, $\Delta(1232)$, $S_{11}(1535)$, and $D_{13}(1520)$ resonance contributions in the blob of Fig. 2. The nucleon contribution is calculable based on the empirical electromagnetic FFs for the nucleon and for the $N \to \Delta$ transition. We will express the Δ intermediate state contribution in terms of the Δ electromagnetic FFs, and will use a lattice calculation for the latter for an estimate. To estimate the unknown $\Delta \to S_{11}$ and $\Delta \to D_{13}$ electromagnetic transitions, we will use a constituent quark model to relate them to the corresponding FFs for the $N \to S_{11}$ and $N \to D_{13}$ electromagnetic transitions. The latter FFs will be taken from experiment. We will detail these different contributions in the following.

A. Nucleon intermediate state contribution

The contribution to $\hat{W}^{\beta\mu\nu}$, corresponding with the nucleon intermediate state in Fig. 2, is exactly calculable in terms of on-shell γ^*NN and $\gamma^*N\Delta$ vertices as:

$$\hat{W}_N^{\beta\mu\nu}(p',p) = 2\pi\,\delta(W^2 - M_N^2)\,\Gamma^{\beta\mu}_{N\Delta}(p',p_N)$$
$$\times P^{(1/2)}(p_N,M_N)\Gamma^\nu_{NN}(p_N,p), \qquad (42)$$

with $p_N \equiv p + q_1$, where $\Gamma^{\beta\mu}_{N\Delta}$ is as in Eq. (12), and the on-shell γ^*NN vertex Γ^ν_{NN} is given by:

$$\Gamma^\nu_{NN}(p_N,p) \equiv (F_1 + F_2)\gamma^\nu - F_2\frac{(p+p_N)^\nu}{2M_N}, \qquad (43)$$

with $F_1(F_2)$ the Dirac (Pauli) proton FFs respectively. For the nucleon intermediate state contribution, the unpolarized hadronic tensor entering Eqs. (29, 35) for B_n

can be written as:

$$H_N^{\kappa\mu\nu} = 2\pi\,\delta(W^2 - M_N^2)$$
$$\times \mathrm{Tr}\left\{\tilde{\Gamma}_{N\Delta}^{\alpha\kappa}(p',p)\,P_{\alpha\beta}^{(3/2)}(p',M_\Delta)\,\Gamma_{N\Delta}^{\beta\mu}(p',p_N)\right.$$
$$\left.\times P^{(1/2)}(p_N,M_N)\Gamma_{NN}^\nu(p_N,p)P^{(1/2)}(p,M_N)\right\}. \tag{44}$$

B. $\Delta(1232)$ intermediate state contribution

The matrix element of the electromagnetic current operator J^μ between spin $3/2$ states can be decomposed into four multipole transitions: a Coulomb monopole (E0), a magnetic dipole (M1), an electric quadrupole (E2) and a magnetic octupole (M3). We firstly write a Lorentz-covariant decomposition for the on-shell $\gamma^*\Delta\Delta$ vertex which exhibits manifest electromagnetic gauge-invariance as [1]:

$$\langle\Delta(p',\lambda')|J^\mu(0)|\Delta(p,\lambda)\rangle \equiv \bar{u}_\alpha(p',\lambda')\Gamma_{\Delta\Delta}^{\alpha\beta\mu}(p',p)u_\beta(p,\lambda), \tag{45}$$

where λ (λ') are the initial (final) Δ helicities, and where $\Gamma_{\Delta\Delta}^{\alpha\beta\mu}$ is given by:

$$\Gamma_{\Delta\Delta}^{\alpha\beta\mu}(p',p) = -\left[F_1^\Delta g^{\alpha\beta} + F_3^\Delta \frac{q^\alpha q^\beta}{(2M_\Delta)^2}\right]\gamma^\mu$$
$$-\left[F_2^\Delta g^{\alpha\beta} + F_4^\Delta \frac{q^\alpha q^\beta}{(2M_\Delta)^2}\right]\frac{i\sigma^{\mu\nu}q_\nu}{2M_\Delta}, \tag{46}$$

where $q = p' - p$. $F_{1,2,3,4}^\Delta$ are the Δ electromagnetic FFs and depend on Q^2. Note that $F_1^\Delta(0) = e_\Delta$ is the Δ electric charge in units of e (e.g., $e_{\Delta^+} = +1$). For further use we also define the quantity $\tau_\Delta \equiv Q^2/(4M_\Delta^2)$.

A physical interpretation of the four electromagnetic $\Delta \to \Delta$ transitions can be obtained by performing a multipole decomposition [45, 46]. The FFs $F_{1,2,3,4}^\Delta$ can be expressed in terms of the multipole form factors G_{E0}, G_{M1}, G_{E2}, and G_{M3}, as [14]:

$$F_1^\Delta = \frac{1}{1+\tau_\Delta}\left\{G_{E0}^\Delta - \frac{2\tau_\Delta}{3}G_{E2}^\Delta\right.$$
$$\left. +\tau_\Delta\left[G_{M1}^\Delta - \frac{4\tau_\Delta}{5}G_{M3}^\Delta\right]\right\},$$
$$F_2^\Delta = -\frac{1}{1+\tau_\Delta}\left\{G_{E0}^\Delta - \frac{2\tau_\Delta}{3}G_{E2}^\Delta - G_{M1}^\Delta + \frac{4\tau_\Delta}{5}G_{M3}^\Delta\right\},$$
$$F_3^\Delta = \frac{2}{(1+\tau_\Delta)^2}\left\{G_{E0}^\Delta - \left(1+\frac{2\tau_\Delta}{3}\right)G_{E2}^\Delta\right.$$
$$\left. +\tau_\Delta\left[G_{M1}^\Delta - \left(1+\frac{4\tau_\Delta}{5}\right)G_{M3}^\Delta\right]\right\},$$
$$F_4^\Delta = -\frac{2}{(1+\tau_\Delta)^2}\left\{G_{E0}^\Delta - \left(1+\frac{2\tau_\Delta}{3}\right)G_{E2}^\Delta\right.$$
$$\left. -\left[G_{M1}^\Delta - \left(1+\frac{4\tau_\Delta}{5}\right)G_{M3}^\Delta\right]\right\}. \tag{47}$$

At $Q^2 = 0$, the multipole FFs define the charge e_Δ, the magnetic dipole moment μ_Δ, the electric quadrupole moment $\mathcal{Q}_\Delta$, and the magnetic octupole moment $\mathcal{O}_\Delta$ as:

$$e_\Delta = G_{E0}^\Delta(0), \qquad \mu_\Delta = \frac{e}{2M_\Delta}G_{M1}^\Delta(0),$$
$$\mathcal{Q}_\Delta = \frac{e}{M_\Delta^2}G_{E2}^\Delta(0), \qquad \mathcal{O}_\Delta = \frac{e}{2M_\Delta^3}G_{M3}^\Delta(0). \tag{48}$$

The inelastic contribution to $\hat{W}^{\beta\mu\nu}$, corresponding with the $\Delta(1232)$ intermediate state in the blob of Fig. 2, is exactly calculable in terms of on-shell $\gamma^*N\Delta$ and $\gamma^*\Delta\Delta$ electromagnetic vertices as:

$$\hat{W}_\Delta^{\beta\mu\nu}(p',p) = 2\pi\,\delta(W^2 - M_\Delta^2)\,\Gamma_{\Delta\Delta}^{\beta\gamma\mu}(p',p_\Delta)$$
$$\times P_{\gamma\delta}^{(3/2)}(p_\Delta,M_\Delta)\Gamma_{N\Delta}^{\delta\nu}(p_\Delta,p). \tag{49}$$

with $p_\Delta \equiv p + q_1$. This allows us, for the Δ intermediate state contribution, to evaluate the unpolarized hadronic tensor entering Eqs. (29, 35) for B_n as:

$$H_\Delta^{\kappa\mu\nu} = 2\pi\,\delta(W^2 - M_\Delta^2)$$
$$\times \mathrm{Tr}\left\{\tilde{\Gamma}_{N\Delta}^{\alpha\kappa}(p',p)P_{\alpha\beta}^{(3/2)}(p',M_\Delta)\Gamma_{\Delta\Delta}^{\beta\gamma\mu}(p',p_\Delta)\right.$$
$$\left.\times P_{\gamma\delta}^{(3/2)}(p_\Delta,M_\Delta)\Gamma_{N\Delta}^{\delta\nu}(p_\Delta,p)P^{(1/2)}(p,M_N)\right\}. \tag{50}$$

In the following, we will study the sensitivity of B_n to the Δ electromagnetic FFs. For the purpose of obtaining an estimate on the expected size of B_n, we will also directly compare with lattice calculations for the Δ FFs. We will use the results for the hybrid lattice calculation of Ref. [14], which was performed for a pion mass of $m_\pi = 353$ MeV. The lattice results for G_{E0}^Δ, were fitted in Ref. [14] by a dipole parameterization:

$$G_{E0}^\Delta(Q^2) = \frac{1}{\left(1 + Q^2/\Lambda_{E0}^2\right)^2}, \tag{51}$$

with resulting fit value :

$$\Lambda_{E0}^2 = 1.160 \pm 0.078 \text{ GeV}^2. \tag{52}$$

The FFs G_{M1}^Δ and G_{E2}^Δ, were fitted by exponential parameterizations since the expected large Q^2-dependence for these FFs drops stronger than a dipole:

$$G_{M1}^\Delta(Q^2) = G_{M1}^\Delta(0)\,e^{-Q^2/\Lambda_{M1}^2},$$
$$G_{E2}^\Delta(Q^2) = G_{E2}^\Delta(0)\,e^{-Q^2/\Lambda_{E2}^2}. \tag{53}$$

The fit to the lattice calculations found as values [14]:

$$G_{M1}^\Delta(0) = 3.04 \pm 0.24, \quad \Lambda_{M1}^2 = 0.935 \pm 0.122 \text{ GeV}^2,$$
$$G_{E2}^\Delta(0) = -2.06_{-2.35}^{+1.27}, \quad \Lambda_{E2}^2 = 0.54_{-0.25}^{+1.69} \text{ GeV}^2. \tag{54}$$

The magnetic octupole form factor G_{M3}^Δ was found to be compatible with zero within the statistical accuracy obtained in Ref. [14], and will be neglected in our calculation.

C. $S_{11}(1535)$ intermediate state contribution

In this section we consider the contribution to B_n when the intermediate state corresponds with the $S_{11}(1535)$ resonance. The $S_{11}(1535)$ resonance, with mass $M_S = 1.535$ GeV, and quantum numbers $I = 1/2$ and $J^P = 1/2^-$, is the negative parity partner of the nucleon.

A Lorentz-covariant decomposition of the matrix element of the e.m. current operator J^μ for the $\gamma^* N S_{11}$ transition, satisfying manifest e.m. gauge-invariance, can be written as:

$$\langle S_{11}(p_S, \lambda_S)|J^\mu(0)|N(p, \lambda)\rangle$$
$$\equiv \bar{\psi}(p_S, \lambda_S)\Gamma^\mu_{NS}(p_S, p)u(p, \lambda), \tag{55}$$

where ψ is the spinor for the S_{11} field, p_S (λ_S) its four-momentum (helicity) respectively, and where the vertex Γ^μ_{NS} is given by:

$$\Gamma^\mu_{NS}(p_S, p) = F_1^{NS}\left(\gamma^\mu - \gamma \cdot q\, \frac{q^\mu}{q^2}\right)\gamma_5$$
$$+ F_2^{NS}\frac{i\sigma^{\mu\nu}q_\nu}{(M_N + M_S)}\gamma_5, \tag{56}$$

with $q \equiv p_S - p$. The functions $F_{1,2}^{NS}$ are the e.m. FFs for the $\gamma^* N S_{11}$ transition and depend on Q^2.

Equivalently, one can parametrize the $\gamma^* N S_{11}$ transition through two helicity amplitudes $A_{1/2}$ and $S_{1/2}$, which are defined in the S_{11} rest frame. These S_{11} rest frame helicity amplitudes are defined through the following matrix elements of the e.m. current operator:

$$A^{NS}_{1/2} \equiv N_{NS}\langle S_{11}(\vec{0}, +1/2)\,|\,J_\mu \cdot \epsilon^\mu_{\lambda=+1}\,|\,N(-\vec{q}, -1/2)\rangle,$$
$$S^{NS}_{1/2} \equiv N_{NS}\langle S_{11}(\vec{0}, +1/2)\,|\,J^0\,|\,N(-\vec{q}, +1/2)\rangle, \tag{57}$$

where both spinors are chosen to have the indicated spin projections along the z-axis (which is chosen along the virtual photon direction) and where the transverse photon polarization vector entering $A_{1/2}$ is given by $\vec{\epsilon}_{\lambda=+1} = -1/\sqrt{2}(1, i, 0)$. Furthermore in Eq. (57), we introduced the conventional normalization factor

$$N_{NS} \equiv \frac{e}{\sqrt{4M_N(M_S^2 - M_N^2)}}. \tag{58}$$

The helicity amplitudes are also functions of the photon virtuality Q^2 and have been extracted from data on the pion electroproduction process on the proton. Using the empirical parameterizations of the helicity amplitudes $A^{pS}_{1/2}$, and $S^{pS}_{1/2}$ from Ref. [43], which are listed in

Eq. (A.8), the transition FFs can then be obtained as:

$$F_1^{NS} = \frac{Q^2}{\sqrt{2}N_{NS}Q_{NS+}Q^2_{NS-}}$$
$$\times \left\{A^{NS}_{1/2} - (M_S - M_N)\sqrt{2}\left(\frac{2M_S}{Q_{NS+}Q_{NS-}}\right)S^{NS}_{1/2}\right\},$$
$$F_2^{NS} = \frac{(M_S^2 - M_N^2)}{\sqrt{2}N_{NS}Q_{NS+}Q^2_{NS-}}$$
$$\times \left\{A^{NS}_{1/2} + \frac{Q^2}{(M_S - M_N)}\sqrt{2}\left(\frac{2M_S}{Q_{NS+}Q_{NS-}}\right)S^{NS}_{1/2}\right\}, \tag{59}$$

where we generalized the shorthand notation of Eq. (13) as:

$$Q^2_{ij\pm} \equiv Q^2 + (M_i \pm M_j)^2, \tag{60}$$

with $i, j = N, \Delta, S, D$ denoting the N, Δ, S_{11}, D_{13} states in the following.

A Lorentz-covariant decomposition of the matrix element of the e.m. current operator J^μ for the transition $\gamma^* S_{11}\Delta$, satisfying manifest e.m. gauge-invariance, can be written as:

$$\langle S_{11}(p_S, \lambda_S)|J^\mu(0)|\Delta(p_\Delta, \lambda_\Delta)\rangle$$
$$\equiv \bar{\psi}(p_S, \lambda_S)\Gamma^{\alpha\mu}_{\Delta S}(p_S, p_\Delta)u_\alpha(p_\Delta, \lambda_\Delta), \tag{61}$$

where the vertex $\Gamma^{\alpha\mu}_{\Delta S}$ is given by:

$$\Gamma^{\alpha\mu}_{\Delta S}(p_S, p_\Delta) = \frac{1}{Q_{\Delta S-}Q_{\Delta S+}}$$
$$\times \left\{ (q^\alpha \gamma^\mu - \gamma \cdot q\, g^{\alpha\mu})\, M_\Delta\, F_1^{\Delta S}\right.$$
$$+ (q^\alpha P^\mu - q \cdot P\, g^{\alpha\mu})\, F_2^{\Delta S}$$
$$\left.+ (q^\alpha q^\mu - q^2 g^{\alpha\mu})\, F_3^{\Delta S}\right\}, \tag{62}$$

where $P \equiv (p_\Delta + p_S)/2$ and $q \equiv p_S - p_\Delta$. In the definition of Eq. (62), the FFs are defined for the $\Delta^+ \to S_{11}$ transition, and the prefactor $1/(Q_{\Delta S-}Q_{\Delta S+})$ was chosen such that the resulting e.m. FFs $F_{1,2,3}^{\Delta S}$ are dimensionless.

The helicity amplitudes are defined through the following specific matrix elements of the electromagnetic current operator

$$A^{\Delta S}_{-1/2} \equiv N_{\Delta S}\langle S_{11}(\vec{0}, -1/2)\,|\,J_\mu \cdot \epsilon^\mu_{\lambda=+1}\,|\,\Delta(-\vec{q}, -3/2)\rangle,$$
$$A^{\Delta S}_{1/2} \equiv N_{\Delta S}\langle S_{11}(\vec{0}, +1/2)\,|\,J_\mu \cdot \epsilon^\mu_{\lambda=+1}\,|\,\Delta(-\vec{q}, -1/2)\rangle,$$
$$S^{\Delta S}_{1/2} \equiv N_{\Delta S}\langle S_{11}(\vec{0}, +1/2)\,|\,J^0\,|\,\Delta(-\vec{q}, +1/2)\rangle, \tag{63}$$

where the subscripts on the helicity amplitudes indicate the S_{11} spin projections along the z-axis (which is chosen along the virtual photon direction), and where we introduced the normalization factor

$$N_{\Delta S} \equiv \frac{e}{\sqrt{4M_S(M_S^2 - M_\Delta^2)}}. \tag{64}$$

Note that we can relate the above helicity amplitudes $A^{\Delta B}_{\lambda_B}$ for the $\Delta \to B$ transition, in the rest frame of the

baryon resonance B with helicity λ_B, to the corresponding amplitudes $A^{B\Delta}_{\lambda_\Delta}$ for the $B \to \Delta$ transition, in the rest frame of the Δ with helicity λ_Δ, as:

$$A^{B\Delta}_{\lambda_\Delta} = \eta_B \eta_\Delta A^{\Delta B}_{1-\lambda_\Delta}, \tag{65}$$

with η_B, η_Δ the corresponding intrinsic parities.

The relations between the helicity amplitudes of Eq. (63) and the transition FFs for the electromagnetic $\Delta \to S_{11}$ transition can be obtained as:

$$F^{\Delta S}_1 = -\frac{1}{N_{\Delta S} Q_{\Delta S-}} \left[\sqrt{3} A^{\Delta S}_{1/2} - A^{\Delta S}_{-1/2} \right],$$

$$F^{\Delta S}_2 = \frac{1}{N_{\Delta S} Q_{\Delta S-}} \left[\sqrt{3} A^{\Delta S}_{1/2} - A^{\Delta S}_{-1/2} \right] - \frac{(Q^2 + M^2_S - M^2_\Delta)}{N_{\Delta S} Q^2_{\Delta S+} Q_{\Delta S-}} \left[\sqrt{3} A^{\Delta S}_{1/2} + A^{\Delta S}_{-1/2} \right] - \frac{4\sqrt{6} M_\Delta M_S Q^2}{N_{\Delta S} Q^3_{\Delta S+} Q^2_{\Delta S-}} S^{\Delta S}_{1/2},$$

$$F^{\Delta S}_3 = -\frac{1}{2 N_{\Delta S} Q_{\Delta S-}} \left[\sqrt{3} A^{\Delta S}_{1/2} - A^{\Delta S}_{-1/2} \right] + \frac{(Q^2 + M^2_S + 3M^2_\Delta)}{2 N_{\Delta S} Q^2_{\Delta S+} Q_{\Delta S-}} \left[\sqrt{3} A^{\Delta S}_{1/2} + A^{\Delta S}_{-1/2} \right] - \frac{2\sqrt{6} M_\Delta M_S (M^2_S - M^2_\Delta)}{N_{\Delta S} Q^3_{\Delta S+} Q^2_{\Delta S-}} S^{\Delta S}_{1/2}. \tag{66}$$

As the helicity amplitudes $A^{\Delta S}_{-1/2}$, $A^{\Delta S}_{1/2}$, and $S^{\Delta S}_{1/2}$ are not know from experiment, we will estimate them using a non-relativistic quark model, as detailed in the Appendix. The quark model provides relations between the helicity amplitudes for the $\Delta \to S_{11}$ transition and the corresponding ones for the $p \to S_{11}$ and $p \to D_{13}$ transitions, as given by Eqs. (A.5,A.7). For the numerical estimates, we will use these relations and use the empirical results of Eq. (A.8) for the electromagnetic $p \to S_{11}$ and $p \to D_{13}$ helicity amplitudes as input.

The inelastic contribution to $\hat{W}^{\beta\mu\nu}$, corresponding with the $S_{11}(1535)$ intermediate state, can then be expressed in terms of on-shell $\gamma^* N S_{11}$ and $\gamma^* \Delta S_{11}$ vertices as:

$$\hat{W}^{\beta\mu\nu}_{S_{11}}(p', p) = 2\pi \, \delta(W^2 - M^2_S) \, \tilde{\Gamma}^{\beta\mu}_{\Delta S}(p_S, p') \\ \times P^{(1/2)}(p_S, M_S) \Gamma^\nu_{NS}(p_S, p), \tag{67}$$

where the adjoint vertex $\tilde{\Gamma}^{\beta\mu}_{\Delta S} \equiv \gamma^0 \left(\Gamma^{\beta\mu}_{\Delta S} \right)^\dagger \gamma^0$ is given by exactly the same operator as in Eq. (62), with $q = p_S - p'$ in this case denoting the outgoing photon momentum.

This allows us, for the S_{11} intermediate state contribution, to evaluate the unpolarized hadronic tensor entering Eqs. (29, 35) for B_n as:

$$H^{\kappa\mu\nu}_{S_{11}} = 2\pi \, \delta(W^2 - M^2_S) \\ \times \mathrm{Tr} \left\{ \tilde{\Gamma}^{\alpha\kappa}_{N\Delta}(p', p) P^{(3/2)}_{\alpha\beta}(p', M_\Delta) \tilde{\Gamma}^{\beta\mu}_{\Delta S}(p_S, p') \\ \times P^{(1/2)}(p_S, M_S) \Gamma^\nu_{NS}(p_S, p) P^{(1/2)}(p, M_N) \right\}. \tag{68}$$

D. $D_{13}(1520)$ intermediate state contribution

We next consider the contribution to B_n when the intermediate state corresponds with the $D_{13}(1520)$ reso-

nance. This is the lowest mass baryon resonance, with mass $M_D = 1.520$ GeV, which has quantum numbers $I = 1/2$ and $J^P = 3/2^-$.

A Lorentz-covariant decomposition of the matrix element of the e.m. current operator J^μ for the $\gamma^* N D_{13}$ transition, satisfying manifest e.m. gauge-invariance, is given by:

$$\langle D_{13}(p_D, \lambda_D) | J^\mu(0) | N(p, \lambda) \rangle \\ \equiv \bar{\psi}_\alpha(p_D, \lambda_D) \Gamma^{\alpha\mu}_{ND}(p_D, p) u(p, \lambda), \tag{69}$$

with p_D (λ_D) denoting the four-momentum (helicity) of the D_{13} state respectively, where ψ_α is the Rarita-Schwinger spinor for the D_{13} field, and where the vertex $\Gamma^{\alpha\mu}_{ND}$ is given by:

$$\Gamma^{\alpha\mu}_{ND}(p_D, p) = \frac{1}{Q_{ND-} Q_{ND+}} \\ \times \left\{ (q^\alpha \gamma^\mu - q \cdot \gamma g^{\alpha\mu}) M_D F^{ND}_1 \right. \\ + (q^\alpha p_D^\mu - q \cdot p_D \, g^{\alpha\mu}) F^{ND}_2 \\ \left. + (q^\alpha q^\mu - q^2 g^{\alpha\mu}) F^{ND}_3 \right\}, \tag{70}$$

with $q \equiv p_D - p$. In Eq. (70), the prefactor was chosen such that the resulting e.m. FFs $F^{ND}_{1,2,3}$ are dimensionless.

In the same way as we did for the $\gamma^* N S_{11}$ transition above, one can also parametrize the $\gamma^* N D_{13}$ transition through helicity amplitudes in the D_{13} rest frame. For the spin-3/2 resonance, we need three helicity amplitudes $A^{ND}_{3/2}$, $A^{ND}_{1/2}$ and $S^{ND}_{1/2}$, which are defined through the following matrix elements of the e.m. current operator:

$$A^{ND}_{3/2} \equiv N_{ND} \langle D_{13}(\vec{0}, +3/2) | J_\mu \cdot \epsilon^\mu_{\lambda=+1} | N(-\vec{q}, +1/2) \rangle,$$

$$A^{ND}_{1/2} \equiv N_{ND} \langle D_{13}(\vec{0}, +1/2) | J_\mu \cdot \epsilon^\mu_{\lambda=+1} | N(-\vec{q}, -1/2) \rangle,$$

$$S^{ND}_{1/2} \equiv N_{ND} \langle D_{13}(\vec{0}, +1/2) | J^0 | N(-\vec{q}, +1/2) \rangle, \tag{71}$$

with N_{ND} defined, analogously as in Eq. (58), as

$$N_{ND} \equiv \frac{e}{\sqrt{4M_N(M_D^2 - M_N^2)}}. \qquad (72)$$

Using the empirical parameterizations of the helicity amplitudes $A_{3/2}^{pD}$, $A_{1/2}^{pD}$, and $S_{1/2}^{pD}$ from Ref. [43], which are listed in Eq. (A.8), the transition FFs can then be obtained as:

$$F_1^{ND} = \frac{1}{N_{ND}Q_{ND-}}\left\{A_{3/2}^{ND} - \sqrt{3}A_{1/2}^{ND}\right\},$$

$$F_1^{ND} + F_2^{ND} = \frac{1}{N_{ND}Q_{ND+}^2 Q_{ND-}}$$
$$\times \left\{(M_D^2 - M_N^2 - Q^2)\left[A_{3/2}^{ND} + \sqrt{3}A_{1/2}^{ND}\right]\right.$$
$$\left. - \frac{4\sqrt{6}M_D^2 Q^2}{Q_{ND+}Q_{ND-}}S_{1/2}^{ND}\right\},$$

$$F_3^{ND} = -\frac{2M_D^2}{N_{ND}Q_{ND+}^2 Q_{ND-}}\left\{A_{3/2}^{ND} + \sqrt{3}A_{1/2}^{ND}\right.$$
$$\left. + \frac{\sqrt{6}(M_D^2 - M_N^2 - Q^2)}{Q_{ND+}Q_{ND-}}S_{1/2}^{ND}\right\}. \qquad (73)$$

A Lorentz-covariant decomposition for the on-shell $\gamma^*\Delta D_{13}$ vertex which exhibits manifest electromagnetic gauge-invariance as:

$$\langle D_{13}(p_D, \lambda_D)|J^\mu(0)|\Delta(p_\Delta, \lambda_\Delta)\rangle$$
$$\equiv \bar{\psi}_\beta(p_D, \lambda_D)\Gamma_{\Delta D}^{\alpha\beta\mu}(p_D, p_\Delta)u_\alpha(p_\Delta, \lambda_\Delta), \qquad (74)$$

where p_Δ (p_D) are the four-momenta and λ_Δ (λ_D) the helicities of Δ (D_{13}) respectively, and where the vertex $\Gamma_{\Delta D}^{\alpha\beta\mu}$ is given by:

$$\Gamma_{\Delta D}^{\alpha\beta\mu}(p_D, p_\Delta) =$$
$$-\left[F_1^{\Delta D}g^{\alpha\beta} + F_3^{\Delta D}\frac{q^\alpha q^\beta}{(M_\Delta + M_D)^2}\right]\left(\gamma^\mu - \gamma \cdot q \frac{q^\mu}{q^2}\right)\gamma_5$$
$$-\left[F_2^{\Delta D}g^{\alpha\beta} + F_4^{\Delta D}\frac{q^\alpha q^\beta}{(M_\Delta + M_D)^2}\right]\frac{i\sigma^{\mu\nu}q_\nu}{(M_\Delta + M_D)}\gamma_5$$
$$-\frac{F_5^{\Delta D}}{(M_\Delta + M_D)}\left(g^{\alpha\mu}q^\beta - g^{\beta\mu}q^\alpha\right)\gamma_5, \qquad (75)$$

where $q \equiv p_D - p_\Delta$.

Although we will only need on-shell vertices in this work, one can also define consistent vertices for off-shell spin-3/2 particles which satisfy a spin-3/2 gauge invariance, as discussed in Ref. [47, 48], i.e. $(p_\Delta)_\alpha \Gamma_{\Delta D}^{\alpha\beta\mu} = 0$ and $(p_D)_\beta \Gamma_{\Delta D}^{\alpha\beta\mu} = 0$, by replacing $e.g.$ in Eq. (75):

$$g^{\alpha\beta} \to \frac{1}{M_\Delta^2 M_D^2}\left\{p_\Delta^2 p_D^2 g^{\alpha\beta} - p_\Delta^2 p_D^\alpha p_D^\beta - p_D^2 p_\Delta^\alpha p_\Delta^\beta\right.$$
$$\left. + p_\Delta \cdot p_D p_\Delta^\alpha p_D^\beta\right\}, \qquad (76)$$

or

$$q^\alpha q^\beta \to \left(q^\alpha - \frac{q \cdot p_\Delta}{p_\Delta^2}p_\Delta^\alpha\right)\left(q^\beta - \frac{q \cdot p_D}{p_D^2}p_D^\beta\right). \qquad (77)$$

For the $\Delta \to D_{13}$ amplitude, there are five helicity amplitudes, defined by the following matrix elements of the e.m. current operator,

$$A_{3/2}^{\Delta D} \equiv N_{\Delta D}\langle D_{13}(\vec{0}, +3/2)|J_\mu \cdot \epsilon_{\lambda=+1}^\mu|\Delta(-\vec{q}, +1/2)\rangle,$$
$$A_{1/2}^{\Delta D} \equiv N_{\Delta D}\langle D_{13}(\vec{0}, +1/2)|J_\mu \cdot \epsilon_{\lambda=+1}^\mu|\Delta(-\vec{q}, -1/2)\rangle,$$
$$A_{-1/2}^{\Delta D} \equiv N_{\Delta D}\langle D_{13}(\vec{0}, -1/2)|J_\mu \cdot \epsilon_{\lambda=+1}^\mu|\Delta(-\vec{q}, -3/2)\rangle,$$
$$S_{3/2}^{\Delta D} \equiv N_{\Delta D}\langle D_{13}(\vec{0}, +3/2)|J^0|\Delta(-\vec{q}, +3/2)\rangle,$$
$$S_{1/2}^{\Delta D} \equiv N_{\Delta D}\langle D_{13}(\vec{0}, +1/2)|J^0|\Delta(-\vec{q}, +1/2)\rangle, \qquad (78)$$

where $N_{\Delta D}$ is defined as

$$N_{\Delta D} \equiv \frac{e}{\sqrt{4M_D(M_D^2 - M_\Delta^2)}}. \qquad (79)$$

It is also convenient to introduce

$$\tilde{F}_{1,3}^{\Delta D} = F_{1,3}^{\Delta D} + \left(\frac{M_D - M_\Delta}{M_D + M_\Delta}\right)F_{2,4}^{\Delta D}. \qquad (80)$$

The helicity amplitudes for the electromagnetic $\Delta \to D_{13}$ transition are obtained as:

$$A_{3/2}^{\Delta D} = N_{\Delta D}\sqrt{\frac{2}{3}}Q_{\Delta D+}\left\{\tilde{F}_1^{\Delta D} - \frac{Q_{\Delta D-}^2}{2M_\Delta(M_D+M_\Delta)}F_5^{\Delta D}\right\},$$

$$A_{-1/2}^{\Delta D} = N_{\Delta D}\sqrt{\frac{2}{3}}Q_{\Delta D+}\left\{\tilde{F}_1^{\Delta D} + \frac{Q_{\Delta D-}^2}{2M_D(M_D+M_\Delta)}F_5^{\Delta D}\right\},$$

$$A_{1/2}^{\Delta D} = N_{\Delta D}\frac{\sqrt{2}}{6}\frac{Q_{\Delta D+}}{M_\Delta M_D}\left\{2\left(Q^2+M_D^2+M_\Delta^2\right)\tilde{F}_1^{\Delta D} - \frac{Q_{\Delta D+}^2 Q_{\Delta D-}^2}{(M_D+M_\Delta)^2}\tilde{F}_3^{\Delta D} + \frac{(M_D-M_\Delta)Q_{\Delta D-}^2}{(M_D+M_\Delta)}F_5^{\Delta D}\right\},$$

$$S_{3/2}^{\Delta D} = N_{\Delta D}\frac{Q_{\Delta D+}^2 Q_{\Delta D-}}{2M_D Q^2}\left\{-(M_D-M_\Delta)\tilde{F}_1^{\Delta D} + \frac{Q_{\Delta D-}^2}{(M_D+M_\Delta)}F_2^{\Delta D}\right\},$$

$$S_{1/2}^{\Delta D} = N_{\Delta D}\frac{Q_{\Delta D+}^2 Q_{\Delta D-}}{6M_D^2 M_\Delta Q^2}\left\{(Q^2+M_D^2+M_\Delta^2-M_D M_\Delta)\left[-(M_D-M_\Delta)\tilde{F}_1^{\Delta D} + \frac{Q_{\Delta D-}^2}{(M_D+M_\Delta)}F_2^{\Delta D}\right]\right.$$

$$\left. + \frac{Q_{\Delta D+}^2 Q_{\Delta D-}^2}{2(M_D+M_\Delta)^2}\left[(M_D-M_\Delta)\tilde{F}_3^{\Delta D} - \frac{Q_{\Delta D-}^2}{(M_D+M_\Delta)}F_4^{\Delta D}\right] + \frac{Q_{\Delta D-}^2 Q^2}{(M_D+M_\Delta)}F_5^{\Delta D}\right\}. \quad (81)$$

Inverting the relations in Eq. (81) gives

$$\tilde{F}_1^{\Delta D} = \sqrt{\frac{3}{2}}\frac{1}{N_{\Delta D}Q_{\Delta D+}(M_D+M_\Delta)}\left(M_D A_{-1/2}^{\Delta D} + M_\Delta A_{3/2}^{\Delta D}\right),$$

$$F_2^{\Delta D} = \frac{(M_D+M_\Delta)}{N_{\Delta D}Q_{\Delta D+}^2 Q_{\Delta D-}^3}\left\{2M_D Q^2 S_{3/2}^{\Delta D} + \sqrt{\frac{3}{2}}Q_{\Delta D+}Q_{\Delta D-}\frac{(M_D-M_\Delta)}{(M_D+M_\Delta)}\left(M_D A_{-1/2}^{\Delta D} + M_\Delta A_{3/2}^{\Delta D}\right)\right\},$$

$$\tilde{F}_3^{\Delta D} = \sqrt{6}\frac{(M_D+M_\Delta)}{N_{\Delta D}Q_{\Delta D+}^3 Q_{\Delta D-}^2}\left\{M_D\left(Q^2+M_D(M_D+M_\Delta)\right)A_{-1/2}^{\Delta D} + M_\Delta\left(Q^2+M_\Delta(M_D+M_\Delta)\right)A_{3/2}^{\Delta D}\right.$$

$$\left. - \sqrt{3}M_D M_\Delta(M_D+M_\Delta)A_{1/2}^{\Delta D}\right\},$$

$$F_4^{\Delta D} = \frac{2(M_D+M_\Delta)^3}{N_{\Delta D}Q_{\Delta D+}^4 Q_{\Delta D-}^5}\left\{2M_D Q^2\left[(Q^2+M_D^2+M_\Delta^2-M_D M_\Delta)S_{3/2}^{\Delta D} - 3M_\Delta M_D S_{1/2}^{\Delta D}\right]\right.$$

$$+ \sqrt{\frac{3}{2}}Q_{\Delta D+}Q_{\Delta D-}\left[M_D(Q^2+M_D(M_D-M_\Delta))A_{-1/2}^{\Delta D} - M_\Delta(Q^2-M_\Delta(M_D-M_\Delta))A_{3/2}^{\Delta D}\right.$$

$$\left.\left. - \sqrt{3}M_D M_\Delta(M_D-M_\Delta)A_{1/2}^{\Delta D}\right]\right\},$$

$$F_5^{\Delta D} = \sqrt{6}\frac{M_D M_\Delta}{N_{\Delta D}Q_{\Delta D+}Q_{\Delta D-}^2}\left(A_{-1/2}^{\Delta D} - A_{3/2}^{\Delta D}\right). \quad (82)$$

As discussed above for the electromagnetic $\Delta \to S_{11}$ transition, for our numerical estimates we will also use the quark model to relate the helicity amplitudes for the $\Delta \to D_{13}$ transition to the corresponding ones for the $p \to S_{11}$ and $p \to D_{13}$ transitions, as given by Eqs. (A.5,A.7), and use the empirical results of Eq. (A.8) for the latter.

The inelastic contribution to $\hat{W}^{\beta\mu\nu}$, corresponding with the $D_{13}(1520)$ intermediate state, can then be expressed in terms of on-shell $\gamma^* N D_{13}$ and $\gamma^* \Delta D_{13}$ vertices

as:

$$\hat{W}_{D_{13}}^{\beta\mu\nu}(p',p) = 2\pi\,\delta(W^2-M_D^2)\,\tilde{\Gamma}_{\Delta D}^{\beta\gamma\mu}(p_D,p')$$
$$\times P_{\gamma\delta}^{(3/2)}(p_D,M_D)\Gamma_{ND}^{\delta\nu}(p_D,p), \quad (83)$$

where the adjoint vertex $\tilde{\Gamma}_{\Delta D}^{\beta\gamma\mu} \equiv \gamma^0\left(\Gamma_{\Delta D}^{\beta\gamma\mu}\right)^\dagger\gamma^0$ is given by the same operator as in Eq. (75), with $q = p_D - p'$ in this case denoting the outgoing photon momentum, and where in addition the sign of the term proportional to the FF $F_5^{\Delta D}$ is reversed.

This allows us, for the D_{13} intermediate state contribu-

tion, to evaluate the unpolarized hadronic tensor entering Eqs. (29, 35) for B_n as:

$$
\begin{aligned}
H_{D_{13}}^{\kappa\mu\nu} &= 2\pi\,\delta(W^2 - M_D^2)\\
&\times \mathrm{Tr}\left\{\tilde{\Gamma}_{N\Delta}^{\alpha\kappa}(p',p)P_{\alpha\beta}^{(3/2)}(p',M_\Delta)\tilde{\Gamma}_{\Delta D}^{\beta\gamma\mu}(p_D,p')\right.\\
&\left.\times P_{\gamma\delta}^{(3/2)}(p_D,M_D)\Gamma_{ND}^{\delta\nu}(p_D,p)P^{(1/2)}(p,M_N)\right\}.
\end{aligned}
$$
(84)

VI. RESULTS AND DISCUSSION

In this section, we will show estimates for the normal beam SSA using the hadronic model described above, which includes the contributions of N, $\Delta(1232)$, $S_{11}(1535)$, and $D_{13}(1520)$ intermediate states.

To visualize the contributions from different kinematical regions entering Eq. (41) for B_n, we will show density plots of the integrand in

$$
B_n \equiv \int \frac{\mathrm{d}Q_1^2\mathrm{d}Q_2^2}{Q_1^2 Q_2^2}I(Q_1^2,Q_2^2),
$$
(85)

where we defined a dimensionless density function $I(Q_1^2,Q_2^2)$ by separating out the factor $1/(Q_1^2Q_2^2)$ in the integrand of Eq. (41).

Due to the photon virtualities in the denominator, the full integrand of B_n is very strongly peaked towards the quasi-VCS regions, where either Q_1^2 or Q_2^2 becomes of order $\mathcal{O}(m_e^2)$, see Eq. (27), corresponding with the physical situations where the intermediate electron is collinear with either the incident or scattered electrons. Furthermore, when $\sqrt{s}$ approaches the invariant mass W of an intermediate baryon resonance, one also obtains an enhancement as both photons become quasi-real, see Eq. (28). As the integrand is amplified in the region of small Q_1^2 and/or Q_2^2 due to these near singularities, special care is needed when integrating over these regions numerically.

The electromagnetic transition strengths are encoded in the dimensionless density function $I(Q_1^2,Q_2^2)$ in Eq. (85). Using the model for the hadronic tensor outlined in Section V, we show the density functions $I(Q_1^2,Q_2^2)$ for a beam energy $E_e = 0.855$ GeV of the A4@MAMI experiment, in Figs. 4 and 5 for the N and $\Delta(1232)$ intermediate states respectively.

In Fig. 6, we show our result for the angular dependence of B_n for a beam energy $E_e = 1.165$ GeV, corresponding with the Qweak@JLab experiment [38]. We notice from Fig. 6 that the nucleon and Δ intermediate state contributions to B_n are strongly forward peaked. This behavior for the $ep \to e\Delta$ process is unlike the corresponding B_n for the elastic process. The measured value for B_n for the elastic $ep \to ep$ process ranges from a few ppm in the forward angular range to around a hundred ppm in the backward angular range for beam energies below and around 1 GeV [31–37], in good agreement with theoretical TPE expectations [29]. For the inelastic pro-
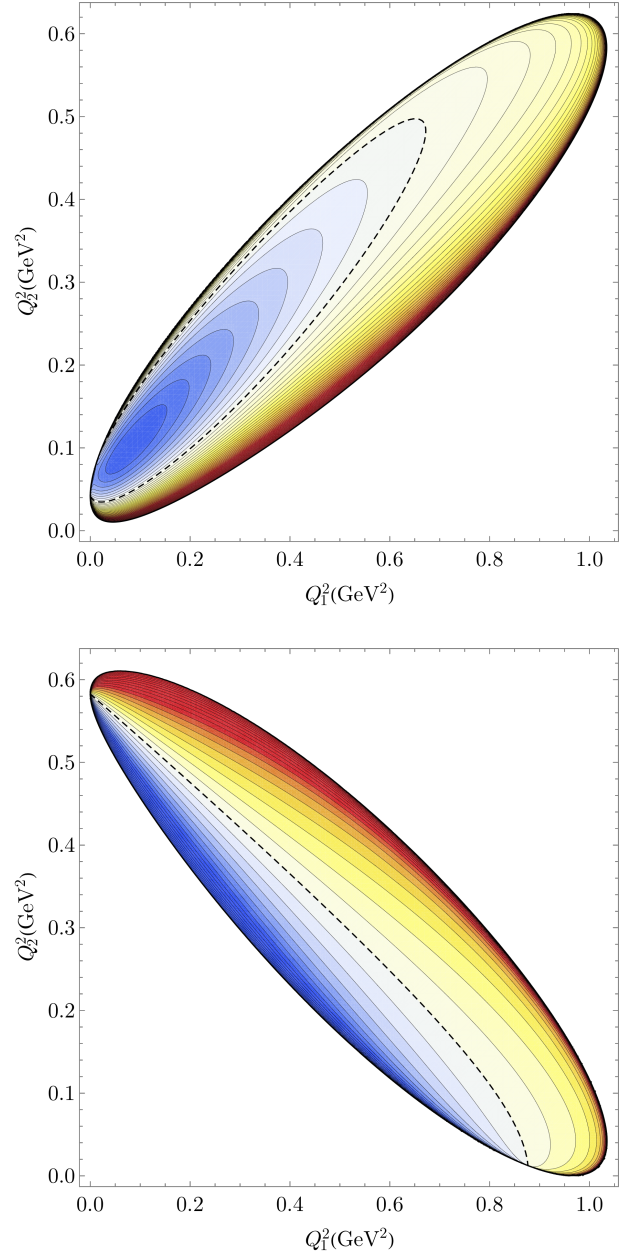

Figure 4. Plot of the density $I(Q_1^2,Q_2^2)$ entering the integrand of B_n in Eq. (85) for the nucleon intermediate state contribution for $E_e = 0.855$ GeV. The upper and lower panels show the distribution for $\theta_{cm} = 30$ deg and $\theta_{cm} = 150$ deg, respectively. The integrand takes zero value along the dashed curve. Larger negative (positive) values of I correspond with stronger shades of blue (red). The distance between the contours corresponds with 0.5×10^{-8} for the upper panel and 1.25×10^{-7} for the bottom panel.

cess $ep \to e\Delta$, we expect an enhancement of B_n in the forward angular range, corresponding with low Q^2, since the OPE process which enters the denominator of B_n, is suppressed by one power of Q^2 relative to its elastic counterpart, as seen from Eqs. (19, 20). We furthermore see from Fig. 6 that the sum of $S_{11}(1535) + D_{13}(1520)$
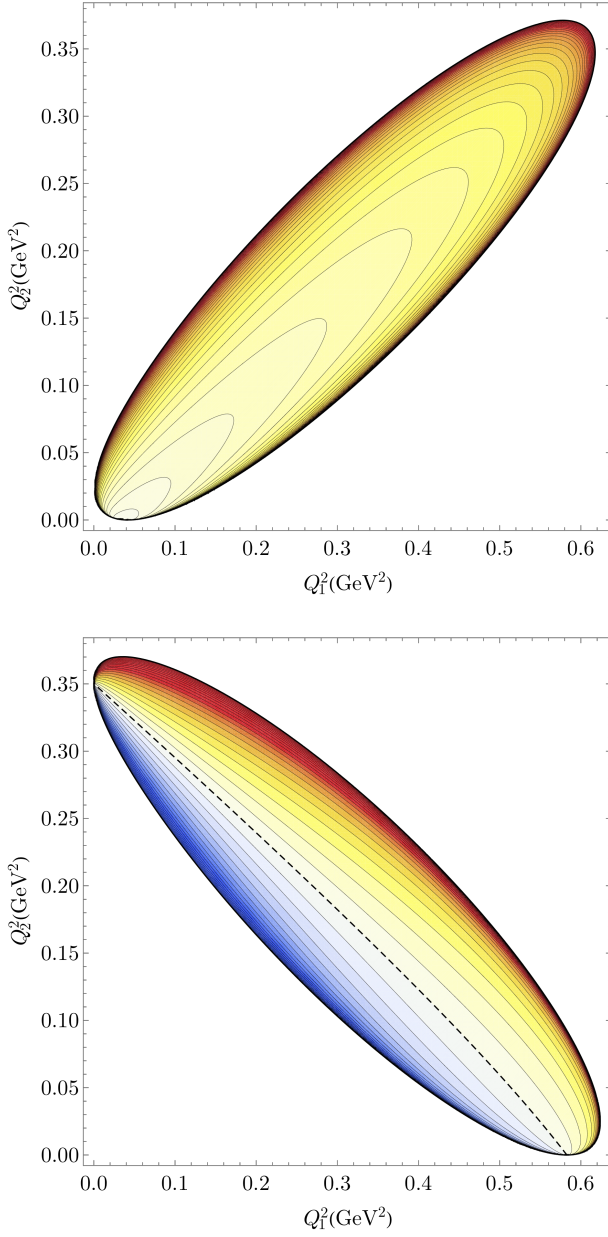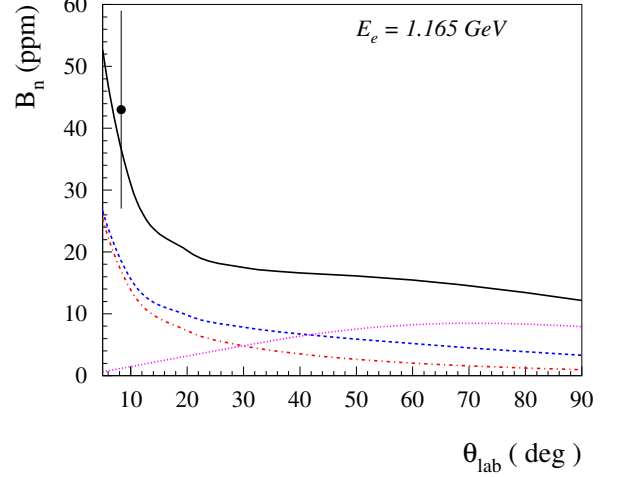
Figure 6. Beam normal spin asymmetry B_n for the $e^-p \to e^-\Delta^+$ process as function of the *lab* scattering angle for a beam energy $E_e = 1.165$ GeV. The curves denote the contributions from different intermediate states: nucleon (dashed-dotted red curve); $\Delta(1232)$ (dashed blue curve); $S_{11}(1535) + D_{13}(1520)$ (dotted violet curve); $N + \Delta + S_{11}(1535) + D_{13}(1520)$ (solid black curve). The data point is from the Qweak Coll. [38].

Figure 5. Plot of the density $I(Q_1^2, Q_2^2)$ entering the integrand of B_n in Eq. (85) for the Δ intermediate state contribution for $E_e = 0.855$ GeV. The upper and lower panels show the distribution for $\theta_{cm} = 30$ deg and $\theta_{cm} = 150$ deg, respectively. The integrand takes zero value along the dashed curve. Larger negative (positive) values of I correspond with stronger shades of blue (red). The distance between the contours corresponds with 0.5×10^{-7} for the upper panel and 0.5×10^{-6} for the bottom panel.

contributions do not show such forward angular enhancement as their electromagnetic transitions are suppressed by an extra momentum transfer. The S_{11} and D_{13} contributions show a similar size and strength, and their combined contribution to B_n becomes larger than the $\Delta(1232)$ contribution for angles $\theta_{\text{lab}} > 45$ deg.

In Fig. 6, we also show a first data point for the beam normal SSA for the $e^-p \to e^-\Delta^+(1232)$ process which has been reported by the Qweak Coll. [38]. Despite its large error bar, the data point at a forward angle of $\theta_{lab} = 8.3$ deg shows a large value of B_n of around 40 ppm for this process. The data point is very well described both in sign and magnitude by our calculation, confirming the large expected enhancement in the forward angular range. Since the $S_{11}(1535) + D_{13}(1520)$ contribution is very small at this angle, B_n is dominated by N and Δ intermediate states at this forward angle. Furthermore, since the $N \to N$, $N \to \Delta$ electromagnetic transitions are well known from experiment, and the $\Delta \to \Delta$ electromagnetic transition is completely dominated by the coupling to the Δ^+ charge at this forward angle, the model dependence in our prediction is very small at this angle.

In Figs. 7 and 8, we show the corresponding results for different kinematics corresponding with the A4@MAMI experiment. Fig. 7 shows the result for $E_e = 0.855$ GeV. This beam energy corresponds with a value $\sqrt{s} \approx 1.58$ GeV, which is closer to the $S_{11}(1535)$ and $D_{13}(1520)$ thresholds. We therefore expect an enhancement of their contributions. As one gets very close to the threshold for an intermediate state contribution, one approaches the situation where the intermediate electron becomes soft, and both photons have small virtualities, see Eq. (28), corresponding with the quasi-real Compton process.

Fig. 8 shows the results for B_n for two beam energies of the A4@MAMI experiment below the thresholds for $S_{11}(1535)$ and $D_{13}(1520)$. These kinematical situ-
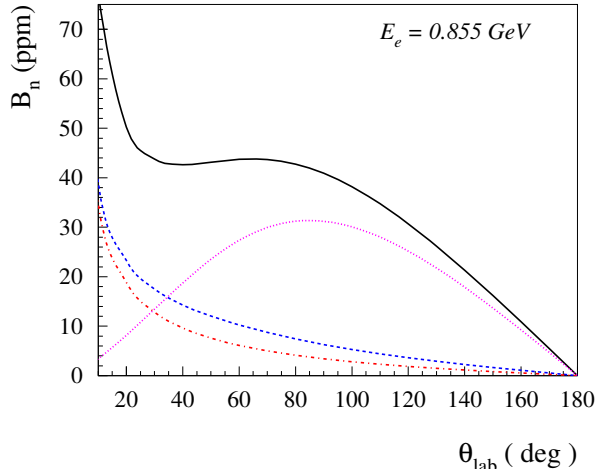
Figure 7. Beam normal spin asymmetry B_n for the $e^-p \to e^-\Delta^+$ process as function of the *lab* scattering angle for a beam energy $E_e = 0.855$ GeV where data have been taken by the A4@MAMI experiment [32, 33]. The curves denote the contributions from different intermediate states: nucleon (dashed-dotted red curve); $\Delta(1232)$ (dashed blue curve); $S_{11}(1535) + D_{13}(1520)$ (dotted violet curve); $N + \Delta + S_{11}(1535) + D_{13}(1520)$ (solid black curve).

ations are therefore dominated by N and Δ intermediate state contributions. We see that the corresponding asymmetries become large at forward angles. In the angular range $\theta_{\text{lab}} = 30 - 40$ deg, where potential data exist from the A4@MAMI experiment, we predict $B_n \simeq 200 - 250$ ppm for $E_e = 0.420$ GeV, and $B_n \simeq 75 - 95$ ppm for $E_e = 0.570$ GeV. It will be interesting to confront these numbers with experiment.

In Fig. 9, we also show the sensitivity of B_n at $E_e = 0.570$ GeV to the value of the Δ^+ magnetic dipole moment μ_Δ. We compare our results for three values of μ_Δ corresponding with the theoretical uncertainty range which is currently listed by PDG, given in Eq. (1). We see from Fig. 9 that for θ_{lab} around $90°$, B_n varies by around 5 ppm when varying μ_Δ in the range $\mu_\Delta = 1.5 - 4.5$ (in units $e/(2M_\Delta)$), in a region where B_n is about 28 ppm.

VII. CONCLUSIONS

In this work, we have presented the general formalism to describe the beam normal spin asymmetry B_n for the $ep \to e\Delta^+(1232)$ process. This beam normal SSA arises from an interference between a one-photon exchange amplitude and the absorptive part of a two-photon exchange amplitude. As the intermediate state in the TPE amplitude is on its mass shell, it allows access to the $\Delta \to \Delta$ and $N^* \to \Delta$ electromagnetic transitions, which otherwise are not accessible in an experiment without resorting to a theory framework. We have provided
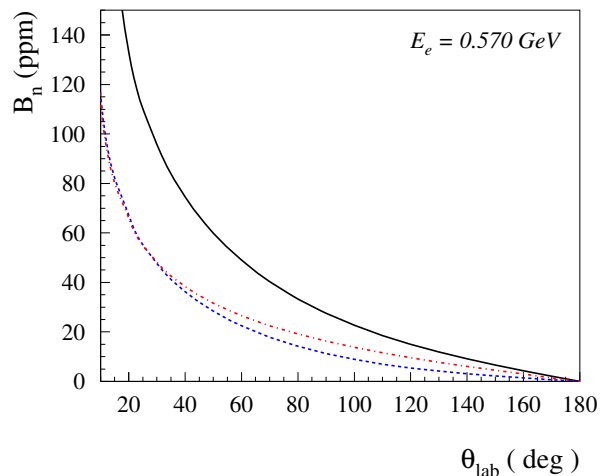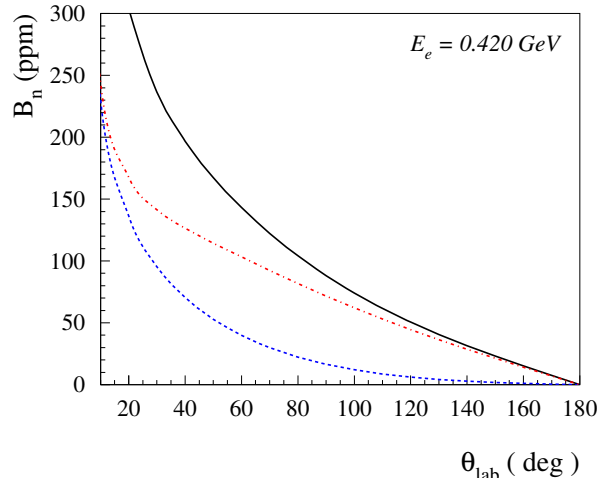

Figure 8. Beam normal spin asymmetry B_n for the $e^-p \to e^-\Delta^+$ process as function of the *lab* scattering angle, for beam energies in the Δ-resonance region where data have been taken by the A4@MAMI experiment [32, 33]. Upper panel: $E_e = 0.420$ GeV; lower panel: $E_e = 0.570$ GeV). The curves denote the contributions from different intermediate states: nucleon (dashed-dotted red curves); $\Delta(1232)$ (dashed blue curves); $N + \Delta$ (solid black curves).

estimates for this asymmetry by considering nucleon, $\Delta(1232)$, $S_{11}(1535)$, and $D_{13}(1520)$ intermediate states. We find that B_n for the $ep \to e\Delta$ process shows a strong enhancement in the forward angular range, as compared to its counterpart for the elastic process $ep \to ep$, which has been measured by several collaborations. The forward enhancement of B_n for the inelastic process is due to the OPE process for the $ep \to e\Delta$ process, entering the denominator of B_n, which is suppressed by one power of Q^2 relative to its elastic counterpart. The normal beam SSA for the $ep \to e\Delta$ reaction therefore offers an in-
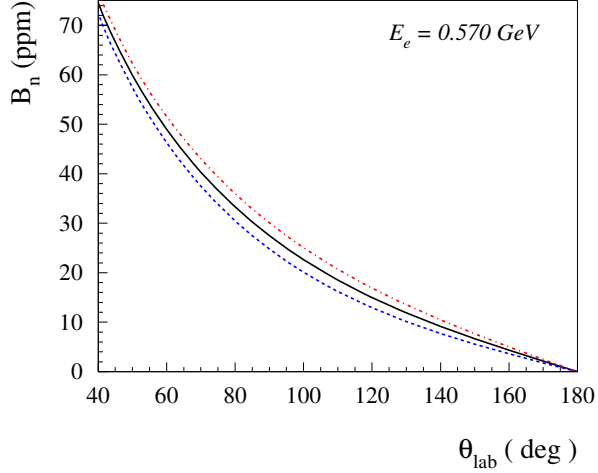
Figure 9. Sensitivity of the beam normal spin asymmetry B_n for the $e^-p \to e^-\Delta^+$ process at $E_e = 0.570$ GeV on the Δ^+ magnetic dipole moment. The curves denote the contributions from $N + \Delta$ intermediate states for different values of μ_Δ (in units of $e/(2M_\Delta)$): $\mu_\Delta = 1.5$ (blue dashed curve); $\mu_\Delta = 3.0$ (black solid curve); $\mu_\Delta = 4.5$ (red dashed-dotted curve).

creased sensitivity to the absorptive part of the TPE amplitude. We have compared our results for B_n with the first data point for the $e^-p \to e^-\Delta^+$ process from the Qweak@JLab experiment and found that the forward angle data point is very well described both in sign and magnitude by our calculation. We have also given predictions for the A4@MAMI experiment, for which data have been taken, and have shown the sensitivity of this observable to the Δ^+ magnetic dipole moment. It will be interesting to analyse those data and provide a comparison with the above theory predictions.

Appendix: Electromagnetic $\Delta \to S_{11}$ and $\Delta \to D_{13}$ transitions in the quark model

For calculations with the S_{11} and D_{13} intermediate states, we need the $\Delta \to S_{11}$ and $\Delta \to D_{13}$ transition matrix elements, as well as the proton to S_{11} and D_{13} matrix elements. The latter are known from analyses of scattering with proton targets [43], but for the former no direct experimental information is available.

However, using ideas from $SU(6)$ or from the constituent quark model one can relate the transition matrix elements involving Δs to those involving nucleons. We shall implement these ideas in a nonrelativistic (NR) limit, and give the helicity amplitudes for the transitions connecting a Δ to the S_{11} or D_{13} in terms of those connecting a proton to the same states. A summary of the techniques and the relevant results are given here. Details regarding the techniques can be found in [49], and the same methods of course can be used for other transitions as well [49–52].

The helicity matrix elements, defined for the present cases in Eqs. (63) and (78), contain the operators $J_\mu \cdot \epsilon^\mu_{\lambda=1}$ and J^0. At the quark level in a NR limit, these operators become

$$J_\mu \cdot \epsilon^\mu_{\lambda=1} \to 3A e_{q3} S_{3+} + 3B e_{q3} L_{3+} \,,$$
$$J^0 \to 3C e_{q3} \,. \tag{A.1}$$

The operators are written in anticipation of use in a wave function completely antisymmetric among the quarks, so we only evaluate for the third quark and multiply by 3; e_{q3} is the charge of the third quark, S_{3+} is the spin raising operator for the third quark, and L_{3+} similarly is the angular momentum raising operator. We have let the photon three-momentum be in the z-direction. The factors A, B, and C depend on position; C is the simplest example being just e^{iqz_3} where z_3 is the z coordinate of the third quark. Details of the derivations may be found in [49] starting from a Hamiltonian formalism, and one can obtain the same results using a NR reduction of standard relativistic expressions for the current.

The Δ state has the same spatial wave function as the nucleon state, and may in short form be given as

$$|\Delta(S_z)\rangle = |\psi^S_{00} \phi^S \chi^S_{S_z}\rangle \,, \tag{A.2}$$

where ψ, ϕ, and χ respectively represent the space, flavor, and spin wave functions of the three quarks, the color wave function is tacit, superscripts S indicate a wave function that is totally symmetric, the subscripts on the space wave function indicate orbital angular momentum and projection, L and L_z, and the subscript on the spin wave function is the spin projection. The flavor wave function, here and elsewhere in this section, is chosen to be for the total charge +1 state.

The states $S_{11}(1535)$ and $D_{13}(1520)$ are negative parity states usually associated with the $SU(6)$ 70-plet states where the three quarks are collectively in a spin-1/2, fla-

vor octet state. Mixing with other states is possible but will be ignored for now. The wave functions, again in short form, are

$$|J, J_z\rangle = \frac{1}{2} \sum_{L_z, S_z} \left(\begin{array}{c|cc} J & 1 & 1/2 \\ J_z & L_z & S_z \end{array} \right)$$
$$\times \left\{ \psi_{1L_z}^{MS} \left(-\phi^{MS}\chi_{S_z}^{MS} + \phi^{MA}\chi_{S_z}^{MA} \right) \right.$$
$$\left. + \psi_{1L_z}^{MA} \left(\phi^{MA}\chi_{S_z}^{MS} + \phi^{MS}\chi_{S_z}^{MA} \right) \right\}, \quad \text{(A.3)}$$

where J is a stand-in for S_{11} when $J = 1/2$ or D_{13} when $J = 3/2$. The first symbol after the summation sign is Clebsch-Gordan coefficient, and superscripts MS and MA stand for mixed symmetry states where the first pair of quarks is either symmetric or antisymmetric.

The crucial matrix elements involving the spatial wave function of the ground state N or Δ on one side and the mixed symmetry states of the 70-plet on the other side are

$$A_1(Q^2) = \langle \psi_{10}^{MS}|A|\psi_{00}^{S}\rangle,$$
$$B_1(Q^2) = \langle \psi_{11}^{MS}|BL_{3+}|\psi_{00}^{S}\rangle,$$
$$C_1(Q^2) = \langle \psi_{10}^{MS}|C|\psi_{00}^{S}\rangle, \quad \text{(A.4)}$$

where A_1, B_1, and C_1 are generally real. The MA states do not enter because of symmetry considerations. Then,

$$A_{1/2}^{\Delta S} = \frac{N_{S\Delta}}{3\sqrt{3}} A_1(Q^2),$$
$$A_{-1/2}^{\Delta S} = -\frac{N_{S\Delta}}{3} A_1(Q^2),$$
$$A_{3/2}^{\Delta D} = 0,$$
$$A_{1/2}^{\Delta D} = -\frac{N_{D\Delta}}{3}\sqrt{\frac{2}{3}} A_1(Q^2),$$
$$A_{-1/2}^{\Delta D} = -\frac{N_{D\Delta}\sqrt{2}}{3} A_1(Q^2). \quad \text{(A.5)}$$

The B amplitudes also do not enter, because of the mismatched spins of the Δ and S_{11}, D_{13} quark wave functions, meaning that the S_{3+} operator is always needed. Similarly, all the scalar S_{11} and D_{13} transition amplitudes to the Δ are zero. Normalizations $N_{S\Delta}$ and $N_{D\Delta}$ are given in Eqs. (64) and (79), respectively.

A pair of proton to 70-plet amplitudes are

$$A_{1/2}^{pS} = \frac{N_{pS}}{\sqrt{6}} \left(-A_1(Q^2) + \sqrt{2}B_1(Q^2) \right),$$
$$A_{1/2}^{pD} = \frac{N_{pD}}{\sqrt{6}} \left(\sqrt{2}A_1(Q^2) + B_1(Q^2) \right). \quad \text{(A.6)}$$

These allow us to obtain A_1 from measured amplitudes,

$$A_1(Q^2) = \sqrt{\frac{2}{3}} \left(\frac{\sqrt{2}A_{1/2}^{pD}}{N_{pD}} - \frac{A_{1/2}^{pS}}{N_{pS}} \right). \quad \text{(A.7)}$$

The MAID parameterizations are [43]:

$$A_{1/2}^{pS} = 66.4 \times 10^{-3} \, \text{GeV}^{-1/2} \left(1 + 1.608 \, Q^2 \right) e^{-0.70Q^2},$$
$$S_{1/2}^{pS} = -2.0 \times 10^{-3} \, \text{GeV}^{-1/2} \left(1 + 23.9 \, Q^2 \right) e^{-0.81Q^2},$$
$$A_{1/2}^{pD} = -27.4 \times 10^{-3} \, \text{GeV}^{-1/2}$$
$$\times \left(1 + 8.580 \, Q^2 - 0.252 \, Q^4 + 0.357 \, Q^8 \right) e^{-1.20Q^2},$$
$$A_{3/2}^{pD} = 160.6 \times 10^{-3} \, \text{GeV}^{-1/2}$$
$$\times \left(1 - 0.820 \, Q^2 + 0.541 \, Q^4 - 0.016 \, Q^8 \right) e^{-1.06Q^2},$$
$$S_{1/2}^{pD} = -63.5 \times 10^{-3} \, \text{GeV}^{-1/2} \left(1 + 4.19 \, Q^2 \right) e^{-3.40Q^2},$$
$$\text{(A.8)}$$

for Q^2 in GeV^2.

[1] V. Pascalutsa, M. Vanderhaeghen and S. N. Yang, Phys. Rept. **437**, 125 (2007).
[2] C. Alexandrou, C. N. Papanicolas and M. Vanderhaeghen, Rev. Mod. Phys. **84**, 1231 (2012).
[3] I. G. Aznauryan *et al.*, Int. J. Mod. Phys. E **22**, 1330015 (2013).
[4] E. E. Jenkins and A. V. Manohar, Phys. Lett. B **335**, 452 (1994).
[5] R. F. Lebed and D. R. Martin, Phys. Rev. D **70**, 016008 (2004).
[6] A. J. Buchmann and R. F. Lebed, Phys. Rev. D **62**, 096005 (2000).
[7] A. J. Buchmann and R. F. Lebed, Phys. Rev. D **67**, 016002 (2003).
[8] G. C. Gellas, T. R. Hemmert, C. N. Ktorides and G. I. Poulis, Phys. Rev. D **60**, 054022 (1999).
[9] V. Pascalutsa and M. Vanderhaeghen, Phys. Rev. Lett.
94, 102003 (2005).
[10] T. A. Gail and T. R. Hemmert, Eur. Phys. J. A **28**, 91 (2006).
[11] M. Procura, Phys. Rev. D **78**, 094021 (2008)
[12] T. Ledwig, J. Martin-Camalich, V. Pascalutsa and M. Vanderhaeghen, Phys. Rev. D **85**, 034013 (2012).
[13] C. Alexandrou *et al.*, Phys. Rev. D **79**, 014507 (2009).
[14] C. Alexandrou, T. Korzec, G. Koutsou, C. Lorce, J. W. Negele, V. Pascalutsa, A. Tsapalis and M. Vanderhaeghen, Nucl. Phys. A **825**, 115 (2009).
[15] C. Aubin, K. Orginos, V. Pascalutsa and M. Vanderhaeghen, Phys. Rev. D **79**, 051502 (2009).
[16] A. I. Machavariani, A. Faessler and A. J. Buchmann, Nucl. Phys. A **646**, 231 (1999) [Erratum-ibid. A **686**, 601 (2001)].
[17] D. Drechsel, M. Vanderhaeghen, M. M. Giannini and E. Santopinto, Phys. Lett. B **484**, 236 (2000).

[18] D. Drechsel and M. Vanderhaeghen, Phys. Rev. C **64**, 065202 (2001).

[19] W. T. Chiang, M. Vanderhaeghen, S. N. Yang and D. Drechsel, Phys. Rev. C **71**, 015204 (2005).

[20] V. Pascalutsa and M. Vanderhaeghen, Phys. Rev. D **77**, 014027 (2008).

[21] M. Kotulla *et al.*, Phys. Rev. Lett. **89**, 272001 (2002).

[22] C. Patrignani *et al.* [Particle Data Group], Chin. Phys. C **40**, no. 10, 100001 (2016).

[23] S. Schumann *et al.*, Eur. Phys. J. A **43**, 269 (2010).

[24] C. E. Carlson and M. Vanderhaeghen, Ann. Rev. Nucl. Part. Sci. **57**, 171 (2007).

[25] A. De Rujula, J. M. Kaplan and E. De Rafael, Nucl. Phys. B **35**, 365 (1971).

[26] Y. W. Zhang *et al.*, Phys. Rev. Lett. **115**, no. 17, 172502 (2015).

[27] A. Afanasev, I. Akushevich and N. P. Merenkov, hep-ph/0208260.

[28] M. Gorchtein, P. A. M. Guichon and M. Vanderhaeghen, Nucl. Phys. A **741**, 234 (2004).

[29] B. Pasquini and M. Vanderhaeghen, Phys. Rev. C **70**, 045206 (2004).

[30] K. S. Kumar, S. Mantry, W. J. Marciano and P. A. Souder, Ann. Rev. Nucl. Part. Sci. **63**, 237 (2013).

[31] S. P. Wells *et al.* [SAMPLE Collaboration], Phys. Rev. C **63**, 064001 (2001).

[32] F. E. Maas *et al.*, Phys. Rev. Lett. **94**, 082001 (2005).

[33] D. B. Ríos *et al.*, Phys. Rev. Lett. **119**, no. 1, 012501 (2017).

[34] D. S. Armstrong *et al.* [G0 Collaboration], Phys. Rev. Lett. **99**, 092301 (2007).

[35] D. Androic *et al.* [G0 Collaboration], Phys. Rev. Lett. **107**, 022501 (2011).

[36] S. Abrahamyan *et al.* [HAPPEX and PREX Collaborations], Phys. Rev. Lett. **109**, 192501 (2012).

[37] B. P. Waidyawansa [Qweak Collaboration], AIP Conf. Proc. **1560**, 583 (2013).

[38] Nuruzzaman [Qweak Collaboration], arXiv:1510.00449 [nucl-ex].

[39] M. M. Dalton, arXiv:1510.01582 [nucl-ex].

[40] B. Buncher and C. E. Carlson, Phys. Rev. D **93**, no. 7, 074032 (2016).

[41] H. F. Jones and M. D. Scadron, Annals Phys. **81**, 1 (1973).

[42] D. Drechsel, S. S. Kamalov and L. Tiator, Eur. Phys. J. A **34**, 69 (2007).

[43] L. Tiator, D. Drechsel, S. S. Kamalov and M. Vanderhaeghen, Eur. Phys. J. ST **198**, 141 (2011).

[44] P. A. M. Guichon and M. Vanderhaeghen, Prog. Part. Nucl. Phys. **41**, 125 (1998).

[45] H. J. Weber and H. Arenhovel, Phys. Rept. **36**, 277 (1978).

[46] S. Nozawa and D. B. Leinweber, Phys. Rev. D **42**, 3567 (1990).

[47] V. Pascalutsa, Phys. Rev. D **58**, 096002 (1998).

[48] V. Pascalutsa and R. Timmermans, Phys. Rev. C **60**, 042201 (1999).

[49] F. E. Close, "An Introduction to Quarks and Partons," Academic Press/London 1979, 481p

[50] C. E. Carlson and C. D. Carone, Phys. Lett. B **441**, 363 (1998).

[51] B. C. Rislow and C. E. Carlson, Phys. Rev. D **83**, 113007 (2011).

[52] C. E. Carlson and B. C. Rislow, Phys. Rev. D **86**, 035013 (2012).